NUREG/CR-4127
EPRI NP-3987
GEAP-30875
Vol. 1

BWR Full Integral Simulation Test (FIST) Program TRAC-BWR Model Development Volume 1 — Numerical Methods

Prepared by C. L. Heck, J. G. M. Andersen

Nuclear Technology and Fuel Division
General Electric Company

Prepared for
U.S. Nuclear Regulatory Commission

and
Electric Power Research Institute

and
General Electric Company

NUREG/CR-4127
EPRI NP-3987
GEAP-30875
Vol. 1
R2

BWR Full Integral Simulation Test (FIST) Program TRAC-BWR Model Development Volume 1 — Numerical Methods

Manuscript Completed: April 1985
Date Published: November 1985

Prepared by
C. L. Heck, J. G. M. Andersen

Nuclear Technology and Fuel Division
General Electric Company
San Jose, CA 95125

Prepared for
Division of Accident Evaluation
Office of Nuclear Regulatory Research
U.S. Nuclear Regulatory Commission
Washington, D.C. 20555
NRC FIN No. B3014

and
Electric Power Research Institute
3412 Hillview Avenue
Palo Alto, CA 94303

and
Nuclear Technology and Fuel Division
General Electric Company
San Jose, CA 95125

PREVIOUS REPORTS IN BWR FIST SERIES

BWR Full Integral Simulation Test (FIST) Program Test Plan,
J.E. Thompson, General Electric Company, NUREG/CR-2575, September 1983.

BWR Full Integral Simulation Test (FIST) Program Facility Description Report,
A.G. Stephens, General Electric Company, NUREG/CR-2576, September 1984.

BWR Full Integral Simulation Test (FIST) Phase I Test Results,
W.S. Hwang, Md. Alamgir, W.A. Sutherland, General Electric Company,
NUREG/CR-3711, September 1984.

NUREG/CR-4127-1
EPRI-NP-3987-1
GEAP-30875-1
April 1985

BWR FULL INTEGRAL SIMULATION TEST (FIST) PROGRAM

CONTRACT NRC-04-76-215

TRAC-BWR MODEL DEVELOPMENT

VOLUME 1 - NUMERICAL METHODS

C. L. Heck
J. G. M. Andersen

Approved: _____
B. S. Shiralkar, Manager
Transient Methods

Approved: _____
L. L. Myers, Program Manager
External Programs

Approved: _____
G. E. Dix, Manager
Core Methods

Approved: _____
J. E. Wood, Manager
Core and Fuel Technology

NUCLEAR ENERGY BUSINESS OPERATIONS • GENERAL ELECTRIC COMPANY
SAN JOSE, CALIFORNIA 95125

GENERAL ELECTRIC

Abstract

A complete technical basis for implementation of the 3-D fast numerics in TRACB04 is presented. The 3-D fast numerics is a generalization of the predictor/corrector method previously developed for the 1-D components in TRACB.

TABLE OF CONTENTS

TABLES

ILLUSTRATIONS

SUMMARY

TRAC-BWR is a best-estimate code for the analysis of Boiling Water Reactor transients. A major activity in the model development task under the FIST program has been the development of more efficient numerical methods for TRAC-BWR. The objective was to reduce the cost of executing TRAC in terms of computer costs as well as engineering costs. Both of these objectives have been realized.

The efficiency of TRAC-BWR numerical methods has been improved in two ways: an implicit integration technique has been implemented and the overall reliability of code has been significantly improved. The numerical integration technique is based on the predictor/corrector method. In this method a two-step approach is taken; in the first step the discretization in space and time is modified in such a way that the equations are stable for any time step size, but without increasing the matrix size of the equations. In the first step the equations are on a nonconserving form, e.g. mass is not perfectly conserved. A second step is therefore implemented to obtain mass conservation. With this implicit integration method there are no stability restrictions on the time step size and the only constraint is determined by the desired accuracy. The method has been extended to cover the three-dimensional (vessel) component in addition to the one dimensional (pipe) components. For slow transients this easily gives an order of magnitude reduction in the execution time.

The reliability of TRAC has been significantly increased by improving its capability to handle discontinuities. In particular, the so-called water packing phenomenon, which is caused by discontinuities in void fraction and velocities, has been eliminated. With the improved reliability, TRAC is less prone to experience iteration failures. It executes faster and requires less supervision. Consequently, both execution time and engineering time have been reduced.

In summary, as a result of development under the FIST program the cost of executing TRAC-BWR has been significantly reduced, thereby enhancing its usefulness as an analysis tool for BWR transients.

SECTION 1

INTRODUCTION

TRAC (Transient Reactor Analysis Code) was originally developed by Los Alamos National Laboratory for the analysis of pressurized water reactors[3]. Development of a boiling water reactor version was initiated in 1979 as a collaborative effort between General Electric Company and Idaho National Engineering Laboratory (INEL). INEL is the prime contractor for the official NRC TRAC BD series of codes. The work performed by GE has been funded by the USNRC, EPRI and GE under the BWR Refill Reflood and FIST Programs and has been closely coordinated with INEL.

Key features of TRAC are a high degree of modularity and a stable numerical method. TRAC thus provides a framework where models for individual reactor components and physical phenomena can easily be interchanged. Furthermore, the free specification of the geometry allows the simulation of almost any geometry ranging from simple basic phenomena test through system performance tests to complicated reactor systems. Consequently, the TRAC framework is a good base, around which a best estimate BWR code could be developed.

The major tasks in the development of a BWR version of TRAC, which have been addressed under the BWR Full Integral Simulation Test (FIST) Program are:

- Development of the fast numerical method.
- Development of the enhanced boron trnasport model and the two phase level model.
- Evaluation and implementation of models for the balance of plant components, such as the turbine, the heat exchanger, and the containment. The treatment of air as an additional field (needed for the conatinment component) and the generalized heat transfer between components have also been included.

Early in the development of TRAC-BWR the main emphasis was on the development of accurate models for the thermal/hydraulic phenomena in the Boiling Water Reactor (BWR). During this phase the existing semi-implicit numeris with its Courant limited time step was adequate. However, as this task was completed and application of TRAC-BWR was extended from large break LOCA analysis to small break LOCAs and transients, the longer duration of these events created the need for faster numerics.

At Los Alamos National Laboratory the stability enhancing two-step (SETS) method was developed for TRAC-PF1[3] and at GE under the Refill/Reflood Program a similar predictor/corrector method was developed for TRACB03[1]. These methods for the 1D components led to significant improvements since the most limiting component often was a 1D component, e.g. at a choked flow location. The 3D Vessel component now often became the most limiting component. An attempt was made to overcome this limitation by simulating the vessel by a combination of 1D components. However, the complication of the many 1D components and associated junctions did not produce the desired improvements in efficiency. Furthermore, the 3D effects that exist, particularly in the bypass and upper plenum of the BWR, could not be simulated adequately. Consequently, to overcome this obstacle an effort to generalize the fast numerics to the 3D Vessel component was initiated.

This document describes the fast numerics developed for the 3D Vessel component under the FIST program.

The models described in this report are included in the FIST Program working version of the code, TRACB04, and have been made available to Idaho National Engineering Laboratory (INEL) for inclusion in future TRACBD versions. The work on TRAC-BWR development has been split and interactively defined between GE and INEL. Figure 1-1 shows the relationship between the two parallel efforts and the interactions between the two series of codes.

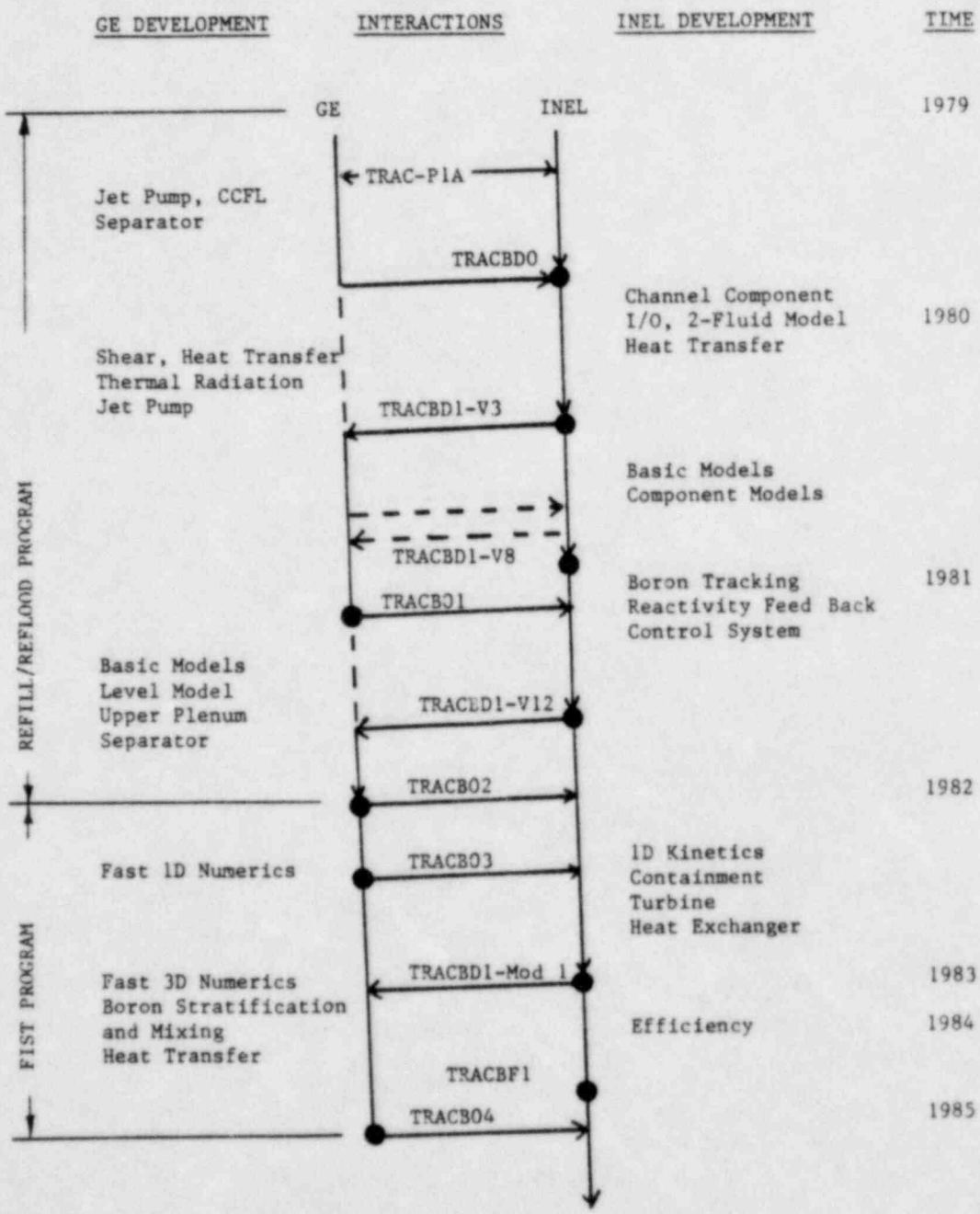

Figure 1-1 Major Milestones in TRAC-BWR Development

SECTION 2

BASIC EQUATIONS

The BWR version of TRAC solves the conservation equations for mass momentum and energy for the gas and liquid phases. The gas phase can be a mixture of steam and air, while no air is assumed to be dissolved in the liquid.

The air and steam in the gas phase are assumed to be perfectly mixed and thus having the same velocity and temperature. Furthermore, Dalton's law applies, i.e.:

$$P_s + P_a = P \tag{2-1}$$

Consequently a total of seven conservation equations are needed: three mass equations for the steam, liquid and air; two momentum equations for the gas and liquid; and two energy equations for the gas and liquid.

The three-dimensional conservation equations are:

Gas mass:

$$\frac{\partial}{\partial t}(\alpha\rho_g) + \nabla \cdot (\alpha\rho_g \overline{V}_g) = \Gamma_g + M_g \tag{2-2}$$

Mixture mass:

$$\frac{\partial}{\partial t}((1-\alpha)\rho_\ell + \alpha\rho_g) + \nabla \cdot ((1-\alpha)\rho_\ell \overline{V}_\ell + \alpha\rho_g \overline{V}_g) = M_m \tag{2-3}$$

Air mass:

$$\frac{\partial}{\partial t}(\alpha\rho_a) + \nabla \cdot (\alpha\rho_a \overline{V}_g) = M_a \tag{2-4}$$

Gas momentum:

$$\frac{\partial}{\partial t}\overline{V}_g + \overline{V}_g \cdot \nabla \overline{V}_g + \frac{k\rho_c}{\alpha\rho_g}\left[\frac{\partial}{\partial t}\overline{V}_R + \overline{V}_d \cdot \nabla \overline{V}_R\right] = \tag{2-5}$$

$$-\frac{1}{\rho_g}\nabla P - \overline{g} - \frac{1}{\alpha\rho_g} f_{\ell g} - \frac{1}{\rho_g} F_w + B_g$$

Liquid momentum:

$$\frac{\partial}{\partial t}(\overline{V}_\ell) + \overline{V}_\ell \cdot \nabla \overline{V}_\ell - \frac{k\rho_c}{(1-\alpha)\rho_\ell}\left[\frac{\partial}{\partial t}\overline{V}_R + \overline{V}_d \cdot \nabla \overline{V}_R\right] =$$

$$-\frac{1}{\rho_\ell}\nabla P - \overline{g} + \frac{1}{(1-\alpha)\rho_\ell} f_{\ell g} - \frac{1}{\rho_\ell} F_w + B_\ell \qquad (2\text{-}6)$$

where $\overline{V}_R = \overline{V}_g - \overline{V}_\ell$ (2-7)

Gas energy:

$$\frac{\partial}{\partial t}(\alpha\rho_g e_g) + \nabla \cdot (\alpha\rho_g e_g \overline{V}_g) + P\left[\frac{\partial \alpha}{\partial t} + \nabla \cdot (\alpha \overline{V}_g)\right] =$$

$$q_{ig} + \Gamma_g h_{gs} + q_{wg} + E_g \qquad (2\text{-}8)$$

Mixture energy:

$$\frac{\partial}{\partial t}((1-\alpha)\rho_\ell e_\ell + \alpha\rho_g e_g) + \nabla \cdot ((1-\alpha)\rho_\ell e_\ell \overline{V}_\ell + \alpha\rho_g e_g \overline{V}_g)$$

$$+ P\nabla \cdot ((1-\alpha)\overline{V}_\ell + \alpha \overline{V}_g) = q_{w\ell} + q_{wg} + E_m \qquad (2\text{-}9)$$

These equations are described in detail in Reference 2 and will not be discussed here. See Section 8 for details of the nomenclature. The primary purpose of this document is to discuss the numerical method used to solve the discretized form of these equations.

2.1 DISCRETIZED BASIC EQUATIONS IN 3 DIMENSIONS

The 3D vessel component in TRAC uses a cylindrical coordinate system as shown in Figure 2-1.

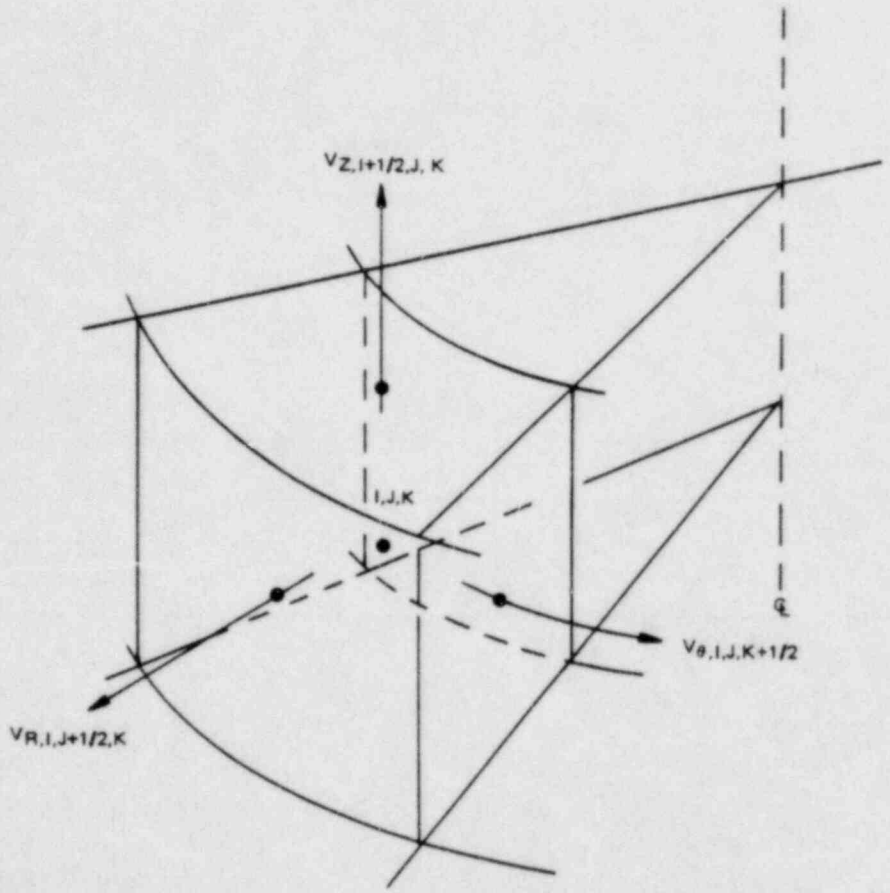

Figure 2-1. CYLINDRICAL COORDINATE SYSTEM WITH STAGGERED GRID

The grid is staggered with the velocities specified at the boundary of each cell and the remaining properties such as α, P, ρ, e specified at the cell center.

Donor cell differencing is used everywhere:

$$V_{i+\frac{1}{2}}\,\phi^{d}_{i+\frac{1}{2}} = V_{i+\frac{1}{2}} \begin{cases} \phi_i & \text{for } V_{i+\frac{1}{2}} \geq 0 \\ \phi_{i+1} & \text{for } V_{i+\frac{1}{2}} < 0 \end{cases} \tag{2-10}$$

$$V_{i+\frac{1}{2}} \left(\frac{\partial V}{\partial X}\right)^{d}_{i+\frac{1}{2}} = V_{i+\frac{1}{2}} \begin{cases} \dfrac{V_{i+\frac{1}{2}} - V_{i-\frac{1}{2}}}{\Delta x} & \text{for } V_{i+\frac{1}{2}} \geq 0 \\ \dfrac{V_{i+3/2} - V_{i-\frac{1}{2}}}{\Delta x} & \text{for } V_{i-\frac{1}{2}} < 0 \end{cases} \tag{2-11}$$

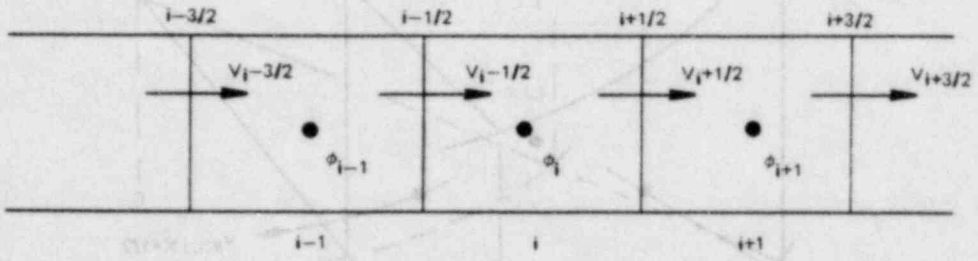

Figure 2-2. STAGGERED GRID VARIABLES

Using this donor cell technique, the discretization will be shown in the following sections.

2.1.1 Discretized Momentum Equations

The momentum equations (2-5) and (2-6) are discretized directly for each face of the cell. Neglecting the offdiagonal terms in the virtual mass, the spacially discretized equations become:

Axial gas momentum:

$$\frac{\partial}{\partial t} V_{gz,\, I+\frac{1}{2},\, J,K} + \left[V_{gz} \left(\frac{\partial V_{gz}}{\partial z}\right)^{d} + V_{gR} \left(\frac{\partial V_{gz}}{\partial R}\right)^{d} + \frac{V_{g\theta}}{R} \left(\frac{\partial V_{gz}}{\partial \theta}\right)^{d}\right]_{I+\frac{1}{2},\, J,K}$$

$$+ \left(\frac{k\rho_c}{\alpha\rho_g}\right)_{I+\frac{1}{2},\, J,K} \left[\frac{\partial}{\partial t} V_{Rz} + V_{dz} \left(\frac{\partial V_{Rz}}{\partial z}\right)^{d}\right]_{I+\frac{1}{2},\, J,K} =$$

$$- \frac{1}{\rho_{g,I+\frac{1}{2},J,K}} \frac{P_{I+1,J,K} - P_{I,J,K}}{\Delta z_{I+\frac{1}{2}}} - \left[g + \frac{1}{\alpha\rho_g} f_{\ell g} + \frac{1}{\rho_g} F_w\right]_{z,I+\frac{1}{2},J,K} + B_{gz,I+\frac{1}{2},J,K} \tag{2-11}$$

Here, if a property is not defined at the face, linear averaging is used, e.g.:

$$\alpha_{I+\frac{1}{2},J,K} = \frac{\Delta z_I \ \alpha_{I,J,K} + \Delta z_{I+1} \ \alpha_{I+1,J,K}}{\Delta z_I + \Delta z_{I+1}}$$

$$V_{g\theta,I+\frac{1}{2},J,K} = \frac{\Delta z_I \left(V_{g\theta,I,J,K-\frac{1}{2}} + V_{g\theta,I,J,K+\frac{1}{2}}\right) + \Delta z_{I+1} \left(V_{g\theta,I+1,J,K-\frac{1}{2}} + V_{g\theta,I+1,J,K+\frac{1}{2}}\right)}{2\left(\Delta z_I + \Delta z_{I+1}\right)}$$

Radial gas momentum:

$$\frac{\partial}{\partial t} V_{gR,I,J+\frac{1}{2},K} + \left[V_{gz} \left(\frac{\partial V_{gR}}{\partial z}\right)^{d} + V_{gR} \left(\frac{\partial V_{gR}}{\partial R}\right)^{d} + \frac{V_{g\theta}}{R} \left(\frac{\partial V_{gR}}{\partial \theta}\right)^{d} - \frac{V_{g\theta}^{2}}{R}\right]_{I,J+\frac{1}{2},K}$$

$$+ \left(\frac{k\rho_c}{\alpha\rho_g}\right)_{I,J+\frac{1}{2},K} \left[\frac{\partial}{\partial t} V_{RR} + V_{dR} \left(\frac{\partial V_{RR}}{\partial R}\right)^{d}\right]_{I,J+\frac{1}{2},K}$$

$$= - \frac{1}{\rho_{g,I,J+\frac{1}{2},K}} \frac{P_{I,J+1,K} - P_{I,J,K}}{\Delta R_{J+\frac{1}{2}}} - \left[\frac{1}{\alpha\rho_g} f_{\ell g} + \frac{1}{\rho_g} F_w\right]_{R,I,J+\frac{1}{2},K}$$

$$+ B_{gR,I,J+\frac{1}{2},K} \tag{2-12}$$

Azimuthal gas momentum:

$$\frac{\partial}{\partial t} V_{g\theta,I,J,K+\frac{1}{2}} + \left[V_{gz} \left(\frac{\partial V_{g\theta}}{\partial z}\right)^{d} + V_{gR} \left(\frac{\partial V_{g\theta}}{\partial R}\right)^{d} + \frac{V_{g\theta}}{R} \left(\frac{\partial V_{g\theta}}{\partial \theta}\right)^{d} + \frac{V_{g\theta} V_{gR}}{R}\right]_{I,J,K+\frac{1}{2}}$$

$$+ \left(\frac{k\rho_c}{\alpha\rho_g}\right)_{I,J,K+\frac{1}{2}} \left[\frac{\partial}{\partial t} V_{R\theta} + \frac{V_{d\theta}}{R} \left(\frac{\partial V_{R\theta}}{\partial \theta}\right)^{d}\right]_{I,J,K+\frac{1}{2}} =$$

$$- \frac{1}{\rho_{g,I,J,K+\frac{1}{2}}} \frac{P_{I,J,K+1} - P_{I,J,K}}{R_{J+\frac{1}{2}} \Delta\theta_{K+\frac{1}{2}}} - \left[\frac{1}{\alpha\rho_g} f_{\ell g} + \frac{1}{\rho_g} F_w\right]_{\theta,I,J,K+\frac{1}{2}}$$

$$+ B_{g\theta,I,J,K+\frac{1}{2}} \qquad (2\text{-}13)$$

Similar expressions exist for the liquid phase.

Axial liquid momentum:

$$\frac{\partial}{\partial t} V_{\ell z,I+\frac{1}{2},J,K} + \left[V_{\ell z} \left(\frac{\partial V_{\ell z}}{\partial z}\right)^{d} + V_{\ell R} \left(\frac{\partial V_{\ell z}}{\partial R}\right)^{d} + \frac{V_{\ell\theta}}{R} \left(\frac{\partial V_{\ell z}}{\partial \theta}\right)^{d}\right]_{I+\frac{1}{2},J,K}$$

$$- \left(\frac{k\rho_c}{(1-\alpha)\rho_\ell}\right)_{I+\frac{1}{2},J,K} \left[\frac{\partial}{\partial t} V_{RZ} + V_{dZ} \left(\frac{\partial V_{RZ}}{\partial Z}\right)^{d}\right]_{I+\frac{1}{2},J,K} =$$

$$\frac{1}{\rho_{\ell,I+\frac{1}{2},J,K}} \frac{P_{I+1,J,K} - P_{I,J,K}}{\Delta z_{I+\frac{1}{2}}} - \left[g - \frac{1}{(1-\alpha)\rho_\ell} f_{\ell g} + \frac{1}{\rho_\ell} F_w\right]_{z,I+\frac{1}{2},J,K}$$

$$+ B_{\ell z,I+\frac{1}{2},J,K} \qquad (2\text{-}14)$$

Radial liquid momentum:

$$\frac{\partial}{\partial t} V_{\ell R,I,J+\frac{1}{2},K} + \left[V_{\ell z} \left(\frac{\partial V_{\ell R}}{\partial z}\right)^{d} + V_{\ell R} \left(\frac{\partial V_{\ell R}}{\partial R}\right)^{d} + \frac{V_{\ell\theta}}{R} \left(\frac{\partial V_{\ell R}}{\partial \theta}\right)^{d} - \frac{V_{\ell\theta}^{2}}{R}\right]_{I,J+\frac{1}{2},K}$$

$$- \left(\frac{k\rho_c}{(1-\alpha)\rho_\ell}\right)_{I,J+\frac{1}{2},K} \left[\frac{\partial}{\partial t} V_{RR} + V_{dR} \left(\frac{\partial V_{RR}}{\partial R}\right)^{d}\right]_{I,J+\frac{1}{2},K} =$$

$$\frac{1}{\rho_{\ell,I,J+\frac{1}{2},K}} \frac{P_{I,J+1,K} - P_{I,J,K}}{\Delta R_{J+\frac{1}{2}}} - \left[\frac{-1}{(1-\alpha)\rho_1} f_{\ell g} + \frac{1}{\rho_\ell} F_w\right]_{I,J+\frac{1}{2},K}$$

$$+ B_{\ell R,I,J+\frac{1}{2},K} \qquad (2\text{-}15)$$

Azimuthal liquid momentum:

$$\frac{\partial}{\partial t} V_{\ell\theta,I,J,K+\frac{1}{2}} + \left[V_{\ell z} \left(\frac{\partial V_{d\theta}}{\partial z}\right)^{d} + V_{\ell R} \left(\frac{\partial V_{\ell\theta}}{\partial R}\right)^{d} + \frac{V_{\ell\theta}}{R} \left(\frac{\partial V_{\ell\theta}}{\partial \theta}\right)^{d} + \frac{V_{\ell\theta} V_{\ell R}}{R}\right]_{I,J,K+\frac{1}{2}}$$

$$- \left(\frac{k\rho_c}{(1-\alpha)\rho_\ell}\right)_{I,J,K+\frac{1}{2}} \left[\frac{\partial}{\partial t} V_{R\theta} + \frac{V_{d\theta}}{R} \left(\frac{\partial V_{R\theta}}{\partial \theta}\right)^{d}\right]_{I,J,K+\frac{1}{2}}$$

$$- \frac{1}{\rho_{\ell,I,J,K+\frac{1}{2}}} \frac{P_{I,J,K+1} - P_{I,J,K}}{R_{J+\frac{1}{2}} \Delta\theta_{K+\frac{1}{2}}} - \left[\frac{-1}{(1-\alpha)\rho_\ell} f_{\ell g} + \frac{1}{\rho_\ell} F_w\right]_{I,J,K+1}$$

$$+ B_{\ell\theta,I,J,K+\frac{1}{2}} \qquad (2\text{-}16)$$

2.1.2 Discretized Mass and Energy Equations

The mass and energy equations are integrated over the volume of the cell to give the total change in mass and energy for the cell.

Gas mass:

$$\Psi_{IJK} \frac{\partial}{\partial t} (\alpha\rho_g)_{IJK} + \sum_{j=1}^{N_f} (A \alpha \rho_g V_g)^{d}_{j,IJK} = \Psi_{IJK} (\Gamma_g + M_g)_{IJK} \qquad (2\text{-}17)$$

Mixture mass:

$$\Psi_{IJK} \frac{\partial}{\partial t} \left((1-\alpha)\rho_\ell + \alpha\rho_g\right)_{IJK} + \sum_{j=1}^{N_f} \left(A(1-\alpha)\rho_\ell V_\ell\right)^{d}_{j,IJK}$$

$$+ \sum_{j=1}^{N_f} (A \alpha \rho_g V_g)_{j,IJK} = \Psi_{IJK} M_{m,IJK} \qquad (2\text{-}18)$$

Air mass:

$$\Psi_{IJK} \frac{\partial}{\partial t} (\alpha\rho_a)_{IJK} + \sum_{j=1}^{N_f} (A\alpha\rho_a V_g)^{d}_{j,IJK} = \Psi_{IJK} M_{a,IJK} \qquad (2\text{-}19)$$

Gas energy:

$$\Psi_{IJK} \frac{\partial}{\partial t} (\alpha\rho_g e_g)_{IJK} + \sum_{j=1}^{N_f} (A \alpha \rho_g e_g V_g)^d_{j,IJK} + \Psi_{IJK} P_{IJK} \left(\frac{\partial\alpha}{\partial t}\right)_{IJK}$$

$$+ P_{IJK} \sum_{j=1}^{N_f} (A \alpha V_g)^d_{j,IJK} = \Psi_{IJK} [q_{ig} + \Gamma_g h_{gs} + q_{wg} + E_g]_{IJK} \qquad (2\text{-}20)$$

Mixture energy:

$$\Psi_{IJK} \frac{\partial}{\partial t} ((1-\alpha)\rho_\ell e_\ell + \alpha \rho_g e_g) + \sum_{j=1}^{N_f} (A (1-\alpha)\rho_\ell e_\ell V_\ell + A \alpha\rho_g e_g V_g)_{j,IJK}$$

$$+ P_{IJK} \sum_{j=1}^{N_f} (A(1-\alpha) V_\ell + A\alpha V_g)_{j,IJK} = \Psi_{IJK} [q_{wl} + q_{wg} + E_m]_{IJK} \qquad (2\text{-}21)$$

In these equations the summation over j indicates the summation over all the faces of the cell.

SECTION 3

PREDICTOR-CORRECTOR METHOD

The predictor-corrector method is a modification of the existing semi-implicit integration method in TRAC. The main principle of the method is to modify the linearization in time in such a way that the equations are numerically stable for time steps in excess of the material Courant limit, but without increasing the size of the matrices to be inverted. This is done in the predictor step; however, perfect conservation of the properties such as mass is not maintained. Therefore the second step, the corrector step, is needed.

To illustrate the principle of the predictor-corrector method consider the following simple system

$$\frac{\partial \phi}{\partial t} = - V \frac{\partial \phi}{\partial x} \tag{3-1}$$

where V is a known velocity with a positive value.

Discretizing Equation (3-1) using a first order explicit method consistent with the existing numerical method in TRAC yields

$$\phi_j^{n+1} - \phi_j^n = - C (\phi_j^n - \phi_{j-1}^n) \tag{3-2}$$

where C is the Courant number: $C = V \frac{\Delta t}{\Delta x}$

This equation can be solved explicitly to give ϕ_i^{n+1}. A stability analysis on this equation gives the following expression for the amplification factor*)

$$\lambda = 1 - C (1-e^{-ik\Delta x}) \tag{3-3}$$

Stability requires $|\lambda| \leq 1$ and consequently we must require $C \leq 1$.

---

*This amplification factor is the growth rate for a disturbance with a wave number k to the solution.

If a fully implicitly integration method was chosen, Equation (3-1) would be linearized as

$$\phi_j^{n+1} - \phi_j^n = - C (\phi_j^{n+1} - \phi_{j-1}^{n+1}) \tag{3-4}$$

A stability analysis on this equation gives

$$\lambda = \frac{1}{1 + C (1-e^{-ik\Delta x})} \tag{3-5}$$

An examination of this equation reveals that $|\lambda| \leq 1$ for all values of C, i.e. the implicit integration method is unconditionally stable. However, from Equation (3-4) it is seen that the fully implicit method requires the inversion of a matrix of size N, where N is the number of mesh cells.

In the predictor step the explicit and implicit integration techniques are combined in such a way that outflow is treated implicitly, but inflow explicitly, and the discretized form of (3-1) becomes

$$\phi_j^{n+1} - \phi_j^n = - C (\phi_j^{n+1} - \phi_{j-1}^n) \tag{3-6}$$

This equation can be solved directly as for the explicit equation and the amplification factor is

$$\lambda = \frac{1 - C\, e^{-ik\Delta x}}{1 + C} \tag{3-7}$$

It is seen that Equation (3-6) is unconditionally stable.

Consequently, in Equation (3-6) we have the simple solution method of the explicit formulation and stability of the implicit formulation. The advantages of both methods are obtained except that the property Φ is not perfectly conserved.

Consider the flow between cell i and i+1. The flow out of cell i is $V\phi_i^{n+i}\ \Delta t$, whereas the flow into cell i+1 is $V\phi_i^n\ \Delta t$ and the error in the conservation of the property ϕ is:

$$E = V\ \Delta t\ (\phi_i^{n+1} - \phi_i^n) = V\ \frac{\partial \phi}{\partial t}\ \Delta t^2 \tag{3-8}$$

The corrector step is needed if perfect conservation of the property ϕ is to be maintained. The exact form of the corrector step depends on the problem to be solved and will be discussed in Section 3.3.

It is worthwhile noting that the error in the property conservation is a second order term, i.e. the same magnitude as the truncation error in any first order integration method.

In the existing semi-implicit integration method in TRAC, the properties convected across a cell face are treated explicitly. The only coupling of new time properties between cells is through the velocity dependence on the pressure difference across the cell faces. The basic form of the equations after elimination of the velocities is:

$$\underline{\underline{A}}_{IJK} \begin{Bmatrix} \Delta P \\ \Delta \alpha \\ \Delta T_g \\ \Delta T_\ell \\ \Delta P_a \end{Bmatrix}_{IJK} = \bar{B}_{IJK} + \sum_{j=1}^{N_f} \bar{C}_{j,IJK}\ \Delta P_{j,IJK} \tag{3-9}$$

where Δ represents the difference between new and old time properties and $\Delta P_{j,IJK}$ is the pressure change in all the neighboring cells. Multiplying this equation with $\underline{\underline{A}}^{-1}_{IJK}$ yields

$$\begin{Bmatrix} \Delta P \\ \Delta \alpha \\ \Delta T_g \\ \Delta T_\ell \\ \Delta P_a \end{Bmatrix}_{IJK} = \underline{\underline{A}}^{-1}_{IJK} \cdot \bar{B}_{IJK} + \sum_{j=1}^{N_f} \underline{\underline{A}}^{-1}_{IJK} \cdot \bar{C}_{j,IJK} \cdot \Delta P_{j,IJK} \tag{3-10}$$

The first row in this matrix equation is the pressure equation, coupling the pressure change in a cell to the pressure changes in the neighboring cells. The pressure equation is a system of linear equations with a size equal to the number of mesh cells in the problem. Consequently, in order to solve the pressure equations, a

N_c x N_c matrix has to be inverted, where N_c is the number of cells. For typical BWR applications N_c is on the order of 100 or less, making this a manageable process.

From Equation (3-10) it is seen that once the pressures are obtained the rest of the properties can be obtained by back substitution.

If a fully implicit formulation was chosen, the convective terms in the conservation equations would depend on the new time step properties in the neighboring cells and Equation (3-9) would become*

$$\underline{\underline{A}}_{IJK} \begin{Bmatrix} \Delta P \\ \Delta\alpha \\ \Delta T_g \\ \Delta T_\ell \\ \Delta P_a \end{Bmatrix}_{IJK} = \overline{B}_{IJK} + \sum_{j=1}^{N_f} \underline{\underline{C}}_{j,IJK} \begin{Bmatrix} \Delta P \\ \Delta\alpha \\ \Delta T_g \\ \Delta T_\ell \\ \Delta P_a \end{Bmatrix}_{j,IJK} \tag{3-11}$$

To solve this equation requires solving a system of equations of size $5N_c$. A comparison of the memory requirement and the number of floating point operations required to solve the equations for the semi-implicit and implicit formulation is given in Table 3-1.

Table 3-1

RESOURCE REQUIREMENTS FOR EXPLICIT AND IMPLICIT METHODS

Method	Memory requirement for coefficient matrix		Floating point operations needed to solve matrix	
	N_c = 50	N_c = 100	N_c = 50	N_c = 100
Semi-implicit	2.5k	10k	0.08M	0.67M
Implicit	62.5k	250k	10.7M	83.8M

*Here a fully implicit formulation of the momentum equations has not been assumed. If this was the case, the vector size would go up by 6.

It is seen that the cost of the implicit formulation would be prohibitive.

The basic principle of the predictor-corrector method is to abandon the requirements of perfect conservation in the predictor step and formulate the convective terms as a combination of old an new time properties, such that outflow from a cell is given by the new properties, but inflow from the neighboring cells is given by the old properties. Consequently, the basic form of the equations would be that of Equation (3-9), the resource requirement would be that of the semi-implicit method, and the stability behavior that of the implicit method.

If a corrector step to restore perfect conservation can be devised, that is not more resource-intensive than the semi-implicit method, the predictor-corrector method has a clear advantage by combining the best features of the semi-implicit and implicit methods. In Section 3.3 it will be shown that this is indeed the case.

3.1 PREDICTOR STEP

The spatial discretization of the 3D conservation equations was shown in Sections 2.1. In this section the discretization in time will be developed. The modification to the existing semi-implicit integration technique to generate the predictor step only affects the temporal discretization.

3.1.1 Momentum Equations

The spatial discretization of the momentum equations was shown in Section 2.1.1. In developing the temporal discretization, let us consider gas and liquid momentum equations for the axial direction, Equations (2-11) and (2-14). As mentioned earlier, the main modification affects the convective terms. In the convective terms the diagonal terms will be calculated using a combination of old and new time properties, such that outflow is given by the new time properties and inflow by the old time properties. The off diagonal terms will be based strictly on old time properties as before. The interfacial shear and wall friction will be based on the new velocities using a Taylor expansion around the old velocities. The fully discretized axial momentum equations then become:

$$V^{n+1}_{gz,I+\frac{1}{2},J,K} - V^{n}_{gz,I+\frac{1}{2},J,K} + \Delta t\, V^{n}_{gz,I+\frac{1}{2},J,K} \begin{cases} \dfrac{V^{n+1}_{gz,I+\frac{1}{2},J,K} - V^{n}_{gz,I-\frac{1}{2},J,K}}{\Delta z_I} & \text{for } V_{gz,I+\frac{1}{2},J,K} \geq 0 \\ \dfrac{V^{n}_{gz,I+3/2,J,K} - V^{n+1}_{gz,I+\frac{1}{2},J,K}}{\Delta z_{I+1}} & \text{for } V_{gz,I+\frac{1}{2},J,K} < 0 \end{cases}$$

$$+ \Delta t \left[V_{gR} \left(\frac{\partial V_{gz}}{\partial R}\right)^{d} + \frac{V_{g\theta}}{R} \left(\frac{V_{gz}}{\partial \theta}\right)^{d} \right]^{n}_{I+\frac{1}{2},J,K}$$

$$+ \left(\frac{k\rho_c}{\alpha\rho_g}\right)^{n}_{I+\frac{1}{2},J,K} \left[V^{n+1}_{Rz} - V^{n}_{Rz} + \Delta t\, V_{dz} \begin{cases} \dfrac{V^{n+1}_{Rz,I+\frac{1}{2}} - V^{n}_{Rz,I-\frac{1}{2}}}{\Delta z_I} & \text{for } V_{dz} \geq o \\ \dfrac{V^{n}_{Rz,I+3/2} - V^{n+1}_{Rz,I+\frac{1}{2}}}{\Delta z_{I+1}} & \text{for } V_{dz} < o \end{cases} \right]_{I+\frac{1}{2},J,K} =$$

$$- \frac{\Delta t}{\rho_{g,I+\frac{1}{2},J,K}} \frac{P^{n+1}_{I+1,J,K} - P^{n+1}_{I,J,K}}{\Delta z_{I+\frac{1}{2}}} - g\Delta t + B^{n}_{gz,I+\frac{1}{2},J,K}\, \Delta t$$

$$- \frac{\Delta t}{(\alpha\rho_g)_{I+\frac{1}{2},J,K}} \left[f^{n}_{\ell g} + \frac{\partial f_{\ell g}}{\partial V_{gz}} (V^{n+1}_{gz} - V^{n}_{gz}) + \frac{\partial f_{\ell g}}{\partial V_{\ell z}} (V^{n+1}_{\ell z} - V^{n}_{\ell z}) \right]_{z,I+\frac{1}{2},J,K}$$

$$- \frac{\Delta t}{\rho_{g,I,J,K}} \left[F^{n}_{w} + \frac{\partial F_w}{\partial V_{gz}} (V^{n+1}_{gz} - V^{n}_{gz}) + \frac{\partial F_w}{\partial V_{\ell z}} (V^{n+1}_{\ell z} - V^{n}_{\ell z}) \right]_{z,I+\frac{1}{2},J,K} \tag{3-12}$$

$$V^{n+1}_{\ell z,I+\frac{1}{2},J,K} - V^{n}_{\ell z,I+\frac{1}{2},J,K} + \Delta t\, V_{\ell z,I+\frac{1}{2},J,K} \begin{cases} \dfrac{V^{n+1}_{\ell z,I+\frac{1}{2},J,K} - V^{n}_{\ell z,I+\frac{1}{2},J,K}}{\Delta z_I} & \text{for } V_{\ell z,I+\frac{1}{2},J,K} \geq o \\ \dfrac{V^{n}_{\ell z,I+3/2,J,K} - V^{n+1}_{\ell z,I+\frac{1}{2},J,K}}{\Delta z_{I+1}} & \text{for } V_{\ell z,I+\frac{1}{2},J,K} < o \end{cases}$$

$$- \Delta t \left[V_{\ell r} \left(\frac{\partial V_{\ell z}}{\partial R}\right)^{d} + \frac{V_{\ell\theta}}{R} \left(\frac{\partial V_{\ell z}}{\partial \theta}\right)^{d} \right]^{n}_{I+\frac{1}{2},J,K}$$

$$- \left(\frac{k\rho_c}{(1-\alpha)\rho_\ell}\right)_{I+\frac{1}{2},J,K} \left[V^{n+1}_{Rz} - V^{n}_{Rz} - \Delta t\, V^{n}_{dz} \begin{cases} \dfrac{V^{n+1}_{Rz,I+\frac{1}{2}} - V^{n}_{Rz,I-\frac{1}{2}}}{\Delta z_I} & \text{for } V_{dz} \geq 0 \\ \dfrac{V^{n}_{Rz,I+3/2} - V^{n}_{Rz,I+\frac{1}{2}}}{\Delta z_{I+1}} & \text{for } V_{dz} < 0 \end{cases} \right]_{I+\frac{1}{2},J,K} =$$

$$- \frac{1}{\rho_{\ell,I+\frac{1}{2},J,K}} \frac{P^{n+1}_{I+1,J,K} - P^{n+1}_{I,J,K}}{\Delta z_{I+\frac{1}{2}}} - g\Delta t + B^{n}_{\ell z,I+\frac{1}{2},J,K}\Delta t$$

$$+ \left(\frac{\Delta t}{(1-\alpha)\rho_\ell}\right)_{I+\frac{1}{2},J,K} \left[f^{n}_{\ell g} + \frac{\partial f_{\ell g}}{\partial V_{gz}} (V^{n+1}_{gz} - V^{n}_{gz}) + \frac{\partial f_{\ell g}}{\partial V_{\ell z}} (V^{n+1}_{\ell z} - V^{n}_{\ell z}) \right]_{z,I+\frac{1}{2},J,K}$$

$$- \frac{\Delta t}{\rho_{\ell,I+\frac{1}{2},J,K}} \left[F^{n}_{w} + \frac{\partial F_w}{\partial V_{gz}} (V^{n+1}_{gz} - V^{n}_{gz}) + \frac{\partial F_w}{\partial V_{\ell z}} (V^{n+1}_{\ell z} - V^{n}_{\ell z}) \right]_{z,I+\frac{1}{2},J,K} \tag{3-13}$$

Examination of these equations reveals that they are linear equations in $V^{n+1}_{gz,I+\frac{1}{2},J,K}$, $V^{n+1}_{\ell z,I+\frac{1}{2},J,K}$, $P^{n+1}_{I,J,K}$ and $P^{n+1}_{I+1,J,K}$. Consequently, the new velocities can be solved for as function of the new pressures.

$$V^{n+1}_{gz,I+\frac{1}{2},J,K} = \hat{V}_{gz,I+\frac{1}{2},J,K} + C_{gz,I+\frac{1}{2},J,K} (P^{n+1}_{I,J,K} - P^{n+1}_{I+1,J,K}) \tag{3-14}$$

$$V^{n+1}_{\ell z,I+\frac{1}{2},J,K} = \hat{V}_{\ell z,I+\frac{1}{2},J,K} + C_{\ell z,I+\frac{1}{2},J,K} (P^{n+1}_{I,J,K} - P^{n+1}_{I+1,J,K}) \tag{3-15}$$

Similar equations can be generated for the radial and azimuthal directions, and for any source connection to the cell.

These equations are then used as shown in the next section to eliminate the velocities from the convective terms in the mass and energy equations.

3.1.2 Mass and Energy Equations

The spatial discretization of the mass and energy equations was shown in Section 2.1.2. As mentioned earlier, the main modification affects the convective terms. In these terms outflow is calculated using new time properties and inflow from a neighboring cell is calculated using old time properties. The heat transfer rates and the vapor generation are based on the new properties. The fully discretized mass and energy equations then become:

Gas Mass

$$\Psi_{IJK}\left[(\alpha\rho_g)^{n+1} - (\alpha\rho_g)^{n}\right]_{IJK} =$$

$$-\left[A_{I+\frac{1}{2},J,K}\, V^{n+1}_{gz,I+\frac{1}{2},J,K}\begin{cases}(\alpha\rho_g)^{n+1}_{I,J,K} & \text{if } V^{n+1}_{gz,I+\frac{1}{2},J,K} \geq 0\\ (\alpha\rho_g)^{n}_{I+1,J,K} & \text{if } V^{n+1}_{gz,I-\frac{1}{2},J,K} < 0\end{cases}\right.$$

$$\left.-A_{I-\frac{1}{2},J,K}\, V^{n+1}_{gz,I-\frac{1}{2},J,K}\begin{cases}(\alpha\rho_g)^{n}_{I-1,J,K} & \text{if } V_{gz,I-\frac{1}{2},J,K} \geq 0\\ (\alpha\rho_g)^{n+1}_{I,J,K} & \text{if } V_{gz,I-\frac{1}{2},J,K} < 0\end{cases}\right]\Delta t$$

+ Similar terms for the J and K directions

$$+\Psi_{IJK}\left(\Gamma^{n+1}_{g} + M^{n+1}_{g}\right)_{IJK}\Delta t \qquad (3\text{-}16)$$

Mixture Mass

$$\Psi_{IJK}\left[((1-\alpha)\rho_\ell + \alpha\rho_g)^{n+1} - ((1-\alpha)\rho_\ell + \alpha\rho_g)^{n}\right]_{IJK} =$$

$$-\left[A_{I+\frac{1}{2},J,K}\, V^{n+1}_{\ell z,I+\frac{1}{2},J,K}\begin{cases}((1-\alpha)\rho_\ell)^{n+1}_{IJK} & \text{for } V^{n+1}_{\ell z,I+\frac{1}{2},J,K} \geq 0\\ ((1-\alpha)\rho_\ell)^{n}_{I+1,J,K} & \text{for } V^{n+1}_{\ell z,I+\frac{1}{2},J,K} < 0\end{cases}\right.$$

$$+A_{I+\frac{1}{2},J,K}\, V^{n+1}_{gz,I+\frac{1}{2},J,K}\begin{cases}(\alpha\rho_g)^{n+1}_{I,J,K} & \text{for } V^{n+1}_{gz,I+\frac{1}{2},J,K} \geq 0\\ (\alpha\rho_g)^{n}_{I+1,J,K} & \text{for } V^{n+1}_{gz,I+\frac{1}{2},J,K} < 0\end{cases}$$

$$-A_{I-\frac{1}{2},J,K}\, V^{n+1}_{\ell z,I-\frac{1}{2},J,K}\begin{cases}((1-\alpha)\rho_\ell)^{n}_{I-1,J,K} & \text{for } V^{n+1}_{\ell z,I-\frac{1}{2},J,K} \geq 0\\ ((1-\alpha)\rho_\ell)^{n+1}_{I,J,K} & \text{for } V^{n+1}_{\ell z,I-\frac{1}{2},J,K} \geq 0\end{cases}$$

$$\left.-A_{I-\frac{1}{2},J,K}\, V^{n+1}_{gz,I-\frac{1}{2},J,K}\begin{cases}(\alpha\rho_g)^{n}_{I-1,J,K} & \text{for } V^{n+1}_{gz,I-\frac{1}{2},J,K} \geq 0\\ (\alpha\rho_g)^{n+1}_{I,J,K} & \text{for } V^{n+1}_{gz,I-\frac{1}{2},J,K} < 0\end{cases}\right]\Delta t$$

+ Similar terms for the J and K directions

$$+\Psi_{IJK}\, M^{n+1}_{m,IJK}\,\Delta t \qquad (3\text{-}17)$$

Air Mass

$$\Psi_{IJK}\ [(\alpha\rho_a)^{n+1} - (\alpha\rho_a)^n]_{IJK} =$$

$$- \left[A_{I+\frac{1}{2},J,K}\ V^{n+1}_{gz,I+\frac{1}{2},J,K} \begin{cases} (\alpha\rho_a)^{n+1}_{I,J,K} & \text{for } V^{n+1}_{gz,I+\frac{1}{2},J,K} \geq o \\ (\alpha\rho_a)^{n}_{I+1,J,K} & \text{for } V^{n+1}_{gz,I+\frac{1}{2},J,K} < o \end{cases} \right.$$

$$\left. - A_{I-\frac{1}{2},J,K}\ V^{n+1}_{gz,I-\frac{1}{2},J,K} \begin{cases} (\alpha\rho_a)^{n}_{I-1,J,K} & \text{for } V^{n+1}_{gz,I-\frac{1}{2},J,K} \geq o \\ (\alpha\rho_a)^{n+1}_{I,J,K} & \text{for } V^{n+1}_{gz,I-\frac{1}{2},J,K} < o \end{cases} \right] \Delta t$$

+ Similar terms for the J and K directions

$$+ \Psi_{IJK}\ M^{n+1}_{a\ IJK}\ \Delta t \qquad (3\text{-}18)$$

Gas Energy

$$\Psi_{IJK}\ [(\alpha\rho_g\ e_g)^{n+1} - (\alpha\rho_g\ e_g)^n + p^{n+1}\ (\alpha^{n+1} - \alpha^n)]_{IJK} =$$

$$- \left[A_{I+\frac{1}{2},J,K}\ V^{n+1}_{gz,I+\frac{1}{2},J,K} \begin{cases} (\alpha\rho_g\ e_g)^{n+1}_{I,J,K} & \text{for } V^{n+1}_{gz,I+\frac{1}{2},J,K} \geq o \\ (\alpha\rho_g\ e_g)^{n}_{I+1,J,K} & \text{for } V^{n+1}_{gz,I+\frac{1}{2},J,K} < o \end{cases} \right.$$

$$\left. - A_{I-\frac{1}{2},J,K}\ V^{n+1}_{gz,I-\frac{1}{2},J,K} \begin{cases} (\alpha\rho_g\ e_g)^{n}_{I-1,J,K} & \text{for } V^{n+1}_{gz,I-\frac{1}{2},J,K} \geq o \\ (\alpha\rho_g\ e_g)^{n+1}_{I,J,K} & \text{for } V^{n+1}_{gz,I-\frac{1}{2},J,K} < o \end{cases} \right] \Delta t$$

+ Similar terms for the J and K directions

$$- p^{n+1}_{IJK} \left[A_{I+\frac{1}{2},J,K}\ V^{n+1}_{gz,I+\frac{1}{2},J,K} \begin{cases} \alpha^{n+1}_{I,J,K} & \text{for } V^{n+1}_{gz,I+\frac{1}{2},J,K} \geq o \\ \alpha^{n}_{I+1,J,K} & \text{for } V^{n+1}_{gz,I+\frac{1}{2},J,K} < o \end{cases} \right.$$

$$\left. - A_{I-\frac{1}{2},J,K}\ V_{gz,I-\frac{1}{2},J,K} \begin{cases} \alpha^{n}_{I-1,J,K} & \text{for } V^{n+1}_{gz,I-\frac{1}{2},J,K} \geq o \\ \alpha^{n+1}_{I,J,K} & \text{for } V^{n+1}_{gz,I-\frac{1}{2},J,K} < o \end{cases} \right] \Delta t$$

+ Similar terms for the J and K directions

$$+ \Psi_{IJK} \left[q_{ig} + \Gamma_g h_{gs} + q_{wg} + E \right]^{n+1}_{g_{IJK}} \Delta t \qquad (3\text{-}19)$$

Mixture Energy

$$\Psi_{IJK} \left[((1-\alpha)\rho_\ell e_\ell + \alpha\rho_g e_g)^{n+1} - ((1-\alpha)\rho_\ell e_\ell + \alpha\rho_g e_g)^n \right]_{IJK} =$$

$$- \left[A_{I+\frac{1}{2},J,K} V^{n+1}_{\ell z, I+\frac{1}{2},J,K} \begin{cases} ((1-\alpha)\rho_\ell e_\ell)^{n+1}_{IJK} + (P(1-\alpha))^{n+1}_{IJK}, \\ \qquad \text{for } V^{n+1}_{\ell z, I+\frac{1}{2},J,K} \geq o \\ ((1-\alpha)\rho_\ell e_\ell)^n_{I+1,J,K} + P^{n+1}_{I,J,K} (1-\alpha)^n_{I+1,J,K}, \\ \qquad \text{for } V^{n+1}_{\ell z, I+\frac{1}{2},J,K} < o \end{cases} \right.$$

$$\left. - A_{I-\frac{1}{2},J,K} V^{n+1}_{\ell z, I-\frac{1}{2},J,K} \begin{cases} ((1-\alpha)\rho_\ell e_\ell)^n_{I-1,J,K} + P^{n+1}_{I,J,K} (1-\alpha)^n_{I-1,J,K} \\ \qquad \text{for } V^{n+1}_{\ell z, I-\frac{1}{2},J,K} \geq o \\ ((1-\alpha)\rho_\ell e_\ell)^{n+1}_{I,J,K} + (P(1-\alpha))^{n+1}_{I,J,K}, \text{ for } V^{n+1}_{\ell z, I-\frac{1}{2},J,K} \geq o \end{cases} \right] \Delta t$$

+ Similar terms for the J and K directions

$$- \left[A_{I+\frac{1}{2},J,K} V^{n+1}_{gz, I+\frac{1}{2},J,K} \begin{cases} (\alpha\rho_g e_g)^{n+1}_{I,J,K} + (P\alpha)^{n+1}_{I,J,K}, \text{ for } V^{n+1}_{gz, I+\frac{1}{2},J,K} \geq o \\ (\alpha\rho_g e_g)^n_{I+1,J,K} + P^{n+1}_{I,J,K} \alpha^n_{I+1,J,K}, \text{ for } V^{n+1}_{gz, I+\frac{1}{2},J,K} < o \end{cases} \right.$$

$$\left. - A_{I-\frac{1}{2},J,K} V^{n+1}_{gz, I-\frac{1}{2},J,K} \begin{cases} (\alpha\rho_g e_g)^n_{I-1,J,K} + P^{n+1}_{I,J,K} \alpha^n_{I-1,J,K}, \text{ for } V^{n+1}_{gz, I-\frac{1}{2},J,K} \geq o \\ (\alpha\rho_g e_g)^{n+1}_{I,J,K} + (P\alpha)^{n+1}_{I,J,K}, \text{ for } V^{n+1}_{gz, I-\frac{1}{2},J,K} \leq o \end{cases} \right] \Delta t$$

+ Similar terms for the J and K directions

$$+ \Psi_{IJK} \left[q_{w\ell} + q_{wg} + E_m \right]^{n+1}_{IJK} \Delta t \qquad (3\text{-}20)$$

Examination of these equations reveals that they are equations in P^{n+1}_{IJK}, α^{n+1}_{IJK}, T^{n+1}_{gIJK}, $T^{n+1}_{\ell IJK}$, P^{n+1}_{aIJK} and the new velocities at the faces of cell IJK. Here the following relationships have been used

$$\rho_g^{n+1} = \rho_g (P^{n+1}, T_g^{n+1}, P_a^{n+1}) \tag{3-21}$$

$$e_g^{n+1} = e_g (P^{n+1}, T_g^{n+1}, P_a^{n+1}) \tag{3-22}$$

$$\rho_\ell^{n+1} = \rho_\ell (P^{n+1}, T_\ell^{n+1}) \tag{3-23}$$

$$e_\ell^{n+1} = e_\ell (P^{n+1}, T_\ell^{n+1}) \tag{3-24}$$

Using Equations (3-14), (3-15) and the equivalent expressions for the radial and azimuthal directions, the new face velocities can be eliminated from Equations (3-16)-(3-20). The resulting equation is of the form

$$\bar{\dot{F}} \left(\begin{Bmatrix} P \\ \alpha \\ T_g \\ T_\ell \\ P_a \end{Bmatrix}^{n+1}_{IJK} \right)_{IJK} + \sum_{j=1}^{N_f} \bar{\dot{F}}_{fj,IJK} (P^{n+1}_{IJK} - P^{n+1}_{j,IJK}) = \bar{S}^{n+1}_{IJK} \tag{3-25}$$

where $\bar{\dot{F}}$ and $\bar{\dot{F}}_f$ are vector functions, and $\bar{S}_{IJK}$ represents the source terms.

$$\bar{S}^{n+1}_{IJK} = \begin{Bmatrix} M_g \\ M_m \\ M_a \\ E_g \\ E_m \end{Bmatrix}^{n+1}_{IJK} \Delta t \tag{3-26}$$

A source term exists for the vessel cell whenever an 1D component is connected to the cell. Using the same discretization technique as for the cell faces, the source terms can be expressed as

$$\Psi M_g = - A_{S,IJK} \; V^{n+1}_{gs,IJK} \begin{cases} (\alpha\rho_g)^{n+1}_{IJK} & \text{for } V^{n+1}_{gs,IJK} \geq o \\ (\alpha\rho_g)^{n}_{S,IJK} & \text{for } V^{n+1}_{gs,IJK} < o \end{cases} \tag{3-27}$$

where the source velocity is measured positive going out and $(\ )_{S,IJK}$ represents the property in the connected 1D cell.

$$\Psi M_m = - A_{S,IJK} \left[V^{n+1}_{\ell s,IJK} \begin{cases} ((1-\alpha)\ \rho_\ell)^{n+1}_{IJK} & \text{for } V^{n+1}_{\ell s,IJK} \geq o \\ ((1-\alpha)\ \rho_\ell)^{n}_{S,IJK} & \text{for } V^{n+1}_{\ell s,IJK} < o \end{cases} \right.$$

$$\left. + V^{n+1}_{gs,IJK} \begin{cases} (\alpha\rho_g)^{n+1}_{IJK} & \text{for } V^{n+1}_{gs,IJK} \geq o \\ (\alpha\rho_g)^{n}_{S,IJK} & \text{for } V^{n+1}_{gs,IJK} < o \end{cases} \right] \tag{3-28}$$

$$\Psi M_a = - A_{s,IJK}\ V^{n+1}_{gs,IJK} \begin{cases} (\alpha\rho_a)^{n+1}_{IJK} & \text{for } V^{n+1}_{gs,IJK} \geq o \\ (\alpha\rho_a)^{n}_{s,IJK} & \text{for } V^{n+1}_{gs,IJK} < o \end{cases} \tag{3-29}$$

$$\Psi E_g = - A_{s,IJK}\ V^{n+1}_{gs,IJK} \begin{cases} (\alpha\rho_g\ e_g)^{n+1}_{IJK} + (P\alpha)^{n+1}_{IJK} & \text{for } V^{n+1}_{gs,IJK} \geq o \\ (\alpha\rho_g\ e_g)^{n}_{s,IJK} + P^{n+1}_{IJK}\ \alpha^{n}_{s,IJK} & \text{for } V^{n+1}_{gs,IJK} < o \end{cases}$$

(3-30)

$$\Psi E_m = - A_{s,IJK} \left[V^{n+1}_{\ell s,IJK} \begin{cases} ((1-\alpha)\ \rho_\ell\ e_\ell)^{n+1}_{IJK} + (P\ (1-\alpha))^{n+1}_{IJK} & \text{for } V^{n+1}_{\ell s,IJK} \geq o \\ ((1-\alpha)\ \rho_\ell\ e_\ell)^{n}_{s,IJK} + P^{n+1}_{IJK}\ (1-\alpha)^{n}_{s,IJK} & \text{for } V^{n+1}_{\ell s,IJK} < o \end{cases} \right.$$

$$\left. + V^{n+1}_{gs,IJK} \begin{cases} (\alpha\rho_g\ e_g)^{n+1}_{IJK} + (P\alpha)^{n+1}_{IJK} & \text{for } V^{n+1}_{gs,IJK} \geq o \\ (\alpha\rho_g\ e_g)^{n}_{s,IJK} + P^{n+1}_{IJK}\ \alpha^{n}_{s,IJK} & \text{for } V^{n+1}_{gs,IJK} < o \end{cases} \right] \tag{3-31}$$

Substituting (3-27)-(3-31) into Equation (3-25) and expressing the source velocities in terms of the pressure difference using expressions equivalent to Equations (3-14) and (3-15) gives

$$\overline{\overline{F}} \left(\begin{Bmatrix} P \\ \alpha \\ T_g \\ T_\ell \\ P_a \end{Bmatrix}^{n+1}_{IJK} \right) + \sum_{j=1}^{N_f} \overline{\overline{F}}_{fj,IJK} \left(P^{n+1}_{IJK} - P^{n+1}_{j,IJK}\right) + \sum_{j=1}^{N_s} \overline{\overline{F}}_{sj} \left(P^{n+1}_{IJK} - P^{n+1}_{sj,IJK}\right) = 0 \tag{3-32}$$

Here a summation over the sources has been introduced for the case that more than one 1D component is connected to the vessel cell.

In solving Equation (3-32) it is convenient to combine P^{n+1}_{IJK} from the second term with the first term. This gives the final form of the discretized mass and energy equations.

$$\bar{F}\left(\begin{Bmatrix} P \\ \alpha \\ T_g \\ T_\ell \\ P_a \end{Bmatrix}^{n+1}_{IJK}\right)_{IJK} + \sum_{j=1}^{N_f} \bar{F}_{fj,IJK}\,(P^{n+1}_{j,IJK}) + \sum_{j=1}^{N_s} \bar{F}_{sj}\,(P^{n+1}_{IJK} - P^{n+1}_{sj,IJK}) = 0 \tag{3-33}$$

The fully discretized mass and energy equations are non-linear equations and are solved using a standard Newton Iteration technique.

$$\underline{\underline{A}}^{m,n+1}_{IJK} \cdot \begin{Bmatrix} \Delta P \\ \Delta\alpha \\ \Delta T_g \\ \Delta T_e \\ \Delta P_a \end{Bmatrix}^{m+1,n+1}_{IJK} = \bar{B}^{m,n+1}_{IJK} + \sum_{j=1}^{N_f} \bar{C}^{m,n+1}_{j,IJK}\,\Delta P^{m+1,n+1}_{j,IJK}$$

$$+ \sum_{j=1}^{N_s} Sc^{m,n+1}_{j,IJK}\,(\Delta P^{m+1,n+1}_{IJK} - \Delta P^{m+1,n+1}_{sj,IJK}) \tag{3-34}$$

where m is the iteration number (this iteration is called the outer iteration). Here $\underline{\underline{A}}_{IJK}$ is the Jacobian matrix of $\bar{F}$

$$\underline{\underline{A}}^{m,n+1}_{IJK} = Ja\,(\bar{F}^{m,n+1}_{IJK}) \tag{3-35}$$

and

$$\bar{C}^{m,n+1}_{j,IJK} = -\frac{\partial \bar{F}^{m,n+1}_{fj,IJK}}{\partial P^{m,n+1}_{j,IJK}} \tag{3-36}$$

$$\bar{Sc}^{m,n+1}_{j,IJK} = -\frac{\partial \bar{F}^{m,n+1}_{sj,IJK}}{\partial\,(P^{m,n+1}_{IJK} - P^{m,n+1}_{sj,IJK})} \tag{3-37}$$

$$\bar{B}^{m,n+1}_{IJK} = -\bar{F}\left(\begin{Bmatrix} P \\ \alpha \\ T_g \\ T_\ell \\ P_a \end{Bmatrix}^{m,n+1}_{IJK}\right)_{IJK} - \sum_{j=1}^{N_f} \bar{F}_{fj,IJK}\,(P^{m,n+1}_{j,IJK}) - \sum_{j=1}^{N_s} \bar{F}_{sj}\,(P^{m,n+1}_{IJK} - P^{m,n+1}_{sj,IJK}) \tag{3-38}$$

Equation (3-34) is the final form of the discretized continuity equations. The solution of this equation will be described in Section 3.2.

3.2 NETWORK SOLUTION

In the previous section, the final discretized form of the conservation equations was developed for the fast numerics. A key feature of this Equation (3-34) is that its basic form is unchanged from the current semi-implicit formulation in TRAC, and only the elements in the equation have been modified, i.e. no new elements have been added and none deleted. Consequently, the existing network solution can be applied without any change. For the sake of completeness, the network solution will be reviewed here.

Multiplying Equation (3-34) by $\underline{\underline{A}}^{-1}_{IJK}$ and omitting the superscript in one gets:

$$\begin{Bmatrix} \Delta P \\ \Delta\alpha \\ \Delta T_g \\ \Delta T_l \\ \Delta P_a \end{Bmatrix}_{IJK} = \bar{\bar{B}}_{IJK} + \sum_{j=1}^{N_f} \bar{\bar{C}}_{j,IJK} \Delta P_{j,IJK} + \sum_{j=1}^{N_s} \bar{\bar{Sc}}_{j,IJK} (\Delta P_{IJK} - \Delta P_{sj,IJK}) \tag{3-39}$$

where

$$\bar{\bar{B}}_{IJK} = \underline{\underline{A}}^{-1}_{IJK} \cdot \bar{\bar{B}}_{IJK} \tag{3-40}$$

$$\bar{\bar{C}}_{J,IJK} = \underline{\underline{A}}^{-1}_{IJK} \cdot \bar{\bar{C}}_{j,IJK} \tag{3-41}$$

$$\bar{\bar{Sc}}_{j,IJK} = \underline{\underline{A}}^{-1}_{IJK} \cdot \bar{\bar{Sc}}_{j,IJK} \tag{3-42}$$

By examination of this equation it is obvious that when all ΔPs are known $\Delta\alpha$, ΔT_g, ΔT_ℓ, and ΔP_a can be obtained through back substitution. Consequently, the task in the network solution reduces to the calculation of the change in total pressure, ΔP.

The first row in Equation (3-39) is

$$\Delta P_{IJK} = \{B_{IJK}\}_1 + \sum_{j=1}^{N_f} \{C_{j,IJK}\}_1 \Delta P_{j,IJK}$$

$$+ \sum_{j=1}^{N_s} \{Sc_{j,IJK}\}_1 (\Delta P_{IJK} - \Delta P_{sj,IJK}) \qquad (3\text{-}43)$$

This is the pressure equation that is solved in the network solution. For an 1D component Equation (3-43) reduces to (see Figure 3-1)

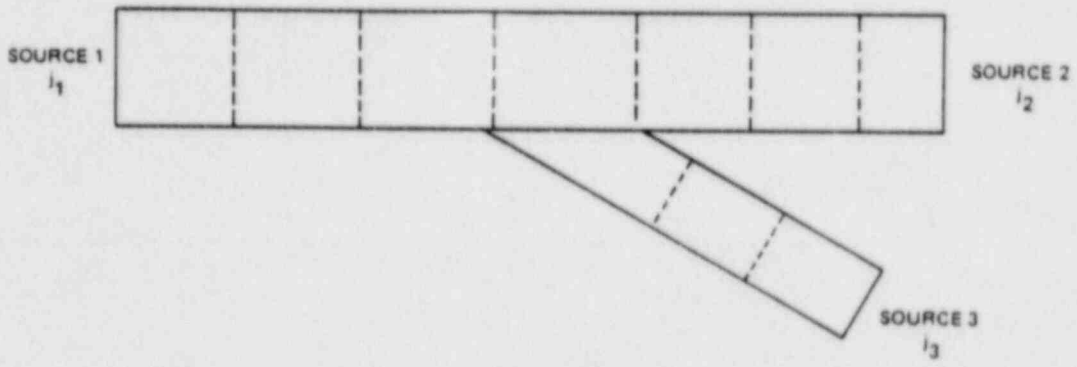

Figure 3-1. NODALIZATION OF 1D COMPONENT

$$\Delta P_i = \{b_i\}_1 + \sum_{j=1}^{N_n} \{c_{j,i}\}_1 \Delta P_{j,i} + \sum_{j=1}^{N_s} \{sc_{j,i}\}_1 (\Delta P_i - \Delta P_{sj,i}) \qquad (3\text{-}44)$$

where

N_n is the number of neighboring cells to any given cell; for an internal cell N_n is 2 or 3; for an end cell N_n is 1;

N_s is the number of sources to a cell; N_s is o for an internal cell; and 1 for an end cell.

Rearranging Equation 3.44 to

$$\Delta P_i - \sum_{j=1}^{N_n} \{c_{j,i}\}_1 \Delta P_{j,i} = \{b_i\}_1 + \sum_{j=1}^{N_s} \{sc_{j,i}\}_1 (\Delta P_i - \Delta P_{sj,i}) \qquad (3\text{-}45)$$

and remembering that $[sc\tilde{}_{i,s}]_1$ is only non-zero for an end cell the, system of linear equations can be solved to give

$$\Delta P_i = d_i + \sum_{s=1}^{N_s} e_{i,s} \Delta^2 P_{js} \tag{3-46}$$

where $\Delta^2 P_{j,s}$ is the change in ΔP across the source junctions

$$\text{e.g.} \qquad \Delta^2 P_{j1} = \Delta P_{j1} - \Delta P_1 \tag{3-47}$$

Let two 1D components be joined together in a junction as shown in Figure (3-2).

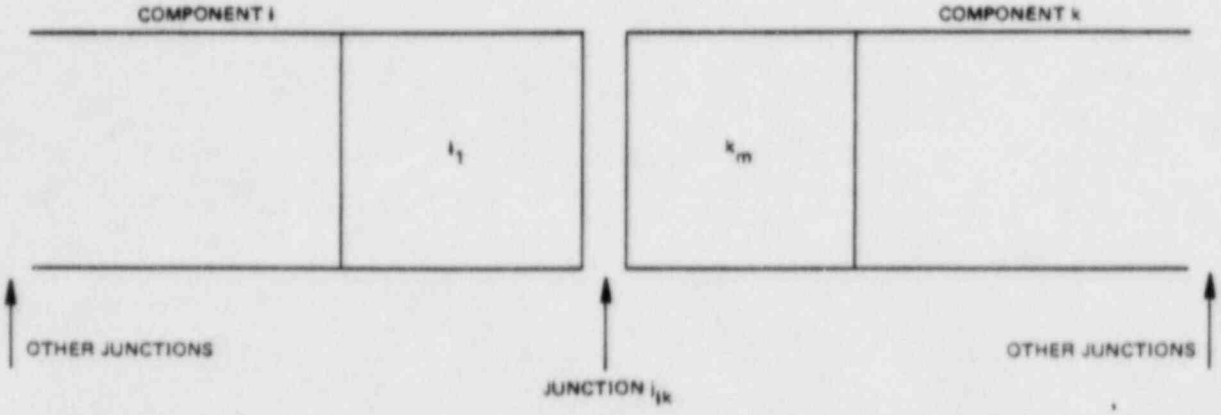

Figure 3-2. JUNCTION OF 1D COMPONENTS

Let $\overline{\Delta^2 P}_j$ be a vector describing ΔP across all junctions in the system including 1D-1D and 1D-3D junctions. For cell i_1, Equation (3-46) can be written as

$$\Delta P_{i1} = d_{i1} + \overline{e}_{i1} \cdot \overline{\Delta^2 P}_j \tag{3-48}$$

Similarly for cell k_m Equation (3-46) can be written as

$$\Delta P_{km} = d_{km} + \overline{e}_{km} \cdot \overline{\Delta^2 P}_j \tag{3-49}$$

Subtracting (3-48) from (3-49) and remembering that

$\Delta^2 P_{jik} = \Delta P_{km} - \Delta P_{i1}$ one gets

$$\Delta^2 P_{jik} = d_{km} - d_{i1} + (\overline{e}_{km} - \overline{e}_{i1}) \cdot \overline{\Delta^2 P}_j \tag{3-50}$$

A 1D component is connected to a 3D component as shown in Figure 3-3.

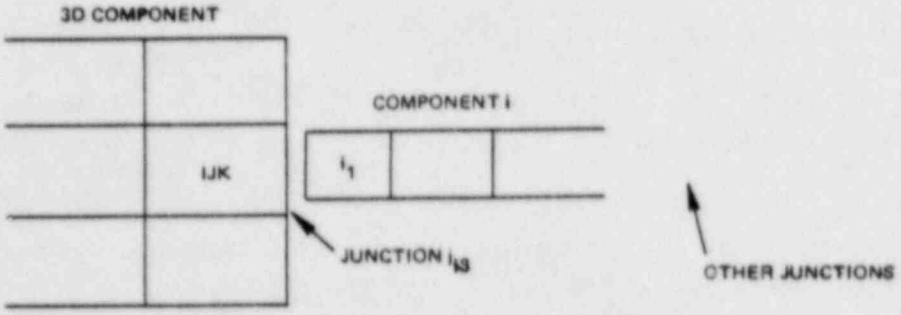

Figure 3-3. JUNCTION OF 1D AND 3D COMPONENTS

For cell i_1 Equation (3-46) can be written as

$$\Delta P_{i1} = d_{i1} + \bar{e}_{i1} \cdot \overline{\Delta^2 P}_j \tag{3-51}$$

Substracting ΔP_{IJK} from this equation and remembering that

$$\Delta^2 P_{ji3} = \Delta P_{i1} - \Delta P_{IJK}$$

$$\Delta^2 P_{ji3} = d_{i1} + \bar{e}_{i1} \cdot \overline{\Delta^2 P}_j - \Delta P_{IJK} \tag{3-52}$$

For all junctions, Equations (3-50) and (3-52) will thus form a system of linear equations:

$$\underline{E} \cdot \overline{\Delta^2 P}_j = \bar{D} + \underline{F} \cdot \overline{\Delta P^3} \tag{3-53}$$

where $\overline{\Delta P^3}$ is a vector of all the pressure changes for the 3D component. Equation (3-53) can be solved to give

$$\overline{\Delta^2 P}_j = \bar{D}' + \underline{F}' \overline{\Delta P^3} \tag{3-54}$$

where: $$\bar{D}' = \underline{E}^{-1} \cdot \bar{D} \tag{3-55}$$

$$\underline{F}' = \underline{E}^{-1} \cdot \underline{F} \tag{3-56}$$

In Equation (3-43) $\Delta P_{IJK} - \Delta P_{IJK,s}$ is ΔP across a junction to a 1D component. Consequently, Equation (3-43) can be written as

$$\underline{G} \cdot \overline{\Delta P^3} = \bar{B}'_1 + \underline{Sc} \cdot \overline{\Delta^2 P}_j \tag{3-57}$$

Substituting Equation (3-54) into this Equation, one gets:

$$\underline{G} \cdot \overline{\Delta P^3} = \overline{B}_1 + \underline{Sc} \cdot [\overline{D} + \underline{F} \cdot \overline{\Delta P^3}] \qquad (3\text{-}58)$$

Equation (3-58) is the final equation in the network solution. It is a system of linear equations that can be solved for pressure changes in the 3D component

From there on the rest of the solution consists of back substitution. $\overline{\Delta^2 P_j}$ is obtained from Equation (3-54), the changes in individual pressures in the 1D components are obtained from Equation (3-46), and finally the changes in α, T_g, T_ℓ and P_a are obtained from Equation (3-39) and its equivalent for the 1D components.

3.3 CORRECTOR STEP

Since new properties are convected out of a node but old properties are convected into the neighboring mode, conservation of properties is not maintained by the predictor step. The goal of the corrector step is to precisely conserve mass. (At this time no attempt is made to precisely conserve energy since simplification of the energy equations makes the energy equations of a non-conserving form[1]; hence, a corrector step to precisely conserve energy is futile.) To conserve mass, the corrector step solves the mixture mass Equation (2-17) to obtain the new void fractions. The mixture mass equation is discretized using a fully implicit technique as:

$$\forall_{IJK} \left[((1-\alpha)\rho_\ell + \alpha\rho_g)^{n+1} - ((1-\alpha)\rho_\ell + \alpha\rho_g)^n\right]_{IJK} =$$

$$- A_{I+\frac{1}{2},J,K} \left[V_{\ell z, I+\frac{1}{2},J,K} \begin{cases} ((1-\alpha)\rho_\ell)^{n+1}_{IJK} & \text{for } V^{n+1}_{\ell z, I+\frac{1}{2},J,K} \geq 0 \\ ((1-\alpha)\rho_\ell)^{n+1}_{I+1,J,K} & \text{for } V^{n+1}_{\ell z, I+\frac{1}{2},J,K} < 0 \end{cases} \right.$$

$$\left. + V^{n+1}_{gz, I+\frac{1}{2},J,K} \begin{cases} (\alpha\rho_g)^{n+1}_{IJK} & \text{for } V^{n+1}_{gz, I+\frac{1}{2},J,K} \geq 0 \\ (\alpha\rho_g)^{n+1}_{I+1,J,K} & \text{for } V^{n+1}_{gz, I+\frac{1}{2},J,K} < 0 \end{cases} \right] \Delta t$$

$$+ A_{I-\frac{1}{2},J,K} \left[V^{n+1}_{\ell z, I-\frac{1}{2},J,K} \begin{cases} ((1-\alpha)\rho_\ell)^{n+1}_{I-1,J,K} & \text{for } V^{n+1}_{\ell z, I-\frac{1}{2},J,K} \geq 0 \\ ((1-\alpha)\rho_\ell)^{n+1}_{I,J,K} & \text{for } V^{n+1}_{\ell z, I-\frac{1}{2},J,K} < 0 \end{cases} \right.$$

$$+ V^{n+1}_{gz,I-\frac{1}{2},J,K} \left\{ \begin{array}{ll} (\alpha\rho_g)^{n+1}_{I-1,J,K} & \text{for } V^{n+1}_{gz,I-\frac{1}{2},J,K} \geq 0 \\ (\alpha\rho_g)^{n+1}_{I,J,K} & \text{for } V^{n+1}_{gz,I-\frac{1}{2},J,K} < 0 \end{array} \right] \Delta t + \Psi_{IJK} M^{n+1}_{m,IJK} \Delta t$$

+ Similar terms for the J and K directions. (3-59)

In this equation, the densities and velocities are those calculated in the predictor for step n+1.

The source term is calculated as indicated in Equation (3-28) but using a fully implicit technique.

$$(\Psi M_m)^{n+1}_{IJK} = -A_{s,IJK} \left[V^{n+1}_{\ell s,IJK} \left\{ \begin{array}{ll} ((1-\alpha)\rho_\ell)^{n+1}_{IJK} & \text{for } V^{n+1}_{\ell s,IJK} \geq 0 \\ ((1-\alpha)\rho_\ell)^{n+1}_{s,IJK} & \text{for } V^{n+1}_{\ell s,IJK} < 0 \end{array} \right. \right.$$

$$\left. + V^{n+1}_{gs,IJK} \left\{ \begin{array}{ll} (\alpha\rho_g)^{n+1}_{IJK} & \text{for } V^{n+1}_{gs,IJK} \geq 0 \\ (\alpha\rho_g)^{n+1}_{s,IJK} & \text{for } V^{n+1}_{gs,IJK} < 0 \end{array} \right] \right. \quad (3-60)$$

Again, the densities and velocities are the new values obtained from the predictor step. Substituting Equation (3-60) into (3-59) gives an equation in only the new void fractions, which can be arranged to be of the form:

$$A_{IJK} \Delta\alpha^{n+1}_{IJK} = B_{IJK} + \sum_{j=1}^{N_f} C_{j,IJK} \Delta\alpha^{n+1}_{j,IJK} \quad (3-61)$$

$$+ \sum_{j=1}^{N_s} Sc_j (\Delta\alpha^{n+1}_{IJK} - \Delta\alpha^{n+1}_{sj,IJK})$$

Dividing this equation with A_{IJK}, gives an equation of exactly the same form as the pressure Equation (3-43) and the network solver can be used unchanged to obtain the new void fractions. Since Equation (3-59) is on a conserving form, the mixture mass is conserved perfectly.

To determine the amount of air relative to steam and to get perfect air conservation, the air mass Equation (2-18) is discretized using a fully implicit technique as:

$$\Psi_{IJK} [m^{n+1}_a - m^n_a]_{IJK} =$$

$$- A_{I+\frac{1}{2},J,K}\left[V^{n+1}_{gz,I+\frac{1}{2},J,K}\begin{cases} m^{n+1}_{aIJK} & \text{for } V^{n+1}_{gz,I+\frac{1}{2},J,K} \geq o \\ m^{n+1}_{aI+1,J,K} & \text{for } V^{n+1}_{gz,I-\frac{1}{2},J,K} \end{cases}\right]\Delta t$$

$$+ A_{I-\frac{1}{2},J,K}\left[V^{n+1}_{gz,I-\frac{1}{2},J,K}\begin{cases} m^{n+1}_{a,I-1,J,K} & \text{for } V^{n+1}_{gz,I-\frac{1}{2},J,K} \geq o \\ m^{n+1}_{a,I,J,K} & \text{for } V^{n+1}_{gz,I-\frac{1}{2},J,K} < o \end{cases}\right]\Delta t$$

+ Similar terms for the J and K directions.

$$+ \Psi_{IJK}\ M^{n+1}_{a,IJK}\ \Delta t \tag{3-62}$$

where $m_a = (\alpha\rho_a)$

The source term is given as

$$\Psi_{IJK}\ M^{n+1}_{a,IJK} = - A_s\ V^{n+1}_{gs,IJK}\begin{cases} m^{n+1}_{a,IJK} & \text{for } V_{gs,IJK} \geq o \\ m^{n+1}_{as,IJK} & \text{for } V_{gs,IJK} < o \end{cases} \tag{3-63}$$

Substituting Equation (3-63) into (3-62) gives an equation in only the new air mass concentration, which can be rearranged to be of the form

$$A_{IJK}\ \Delta m^{n+1}_{a,IJK} = B_{IJK} + \sum_{j=1}^{N_f} C_{j,IJK}\ \Delta m^{n+1}_{aj,IJK} \tag{3-64}$$

$$+ \sum_{j=1}^{N_s} Sc_j\ (\Delta m^{n+1}_{a,IJK} - \Delta m^{n+1}_{asj,IJK})$$

This equation is again of the same form as the pressure Equation (3-43) and the network solver is used unchanged to get the new air concentration.

SECTION 4

WATER PACKING

Water packing is a numerical phenomenon that is introduced by the discretization in space. In order to describe the water packing phenomena, let us consider Figure 4-1.

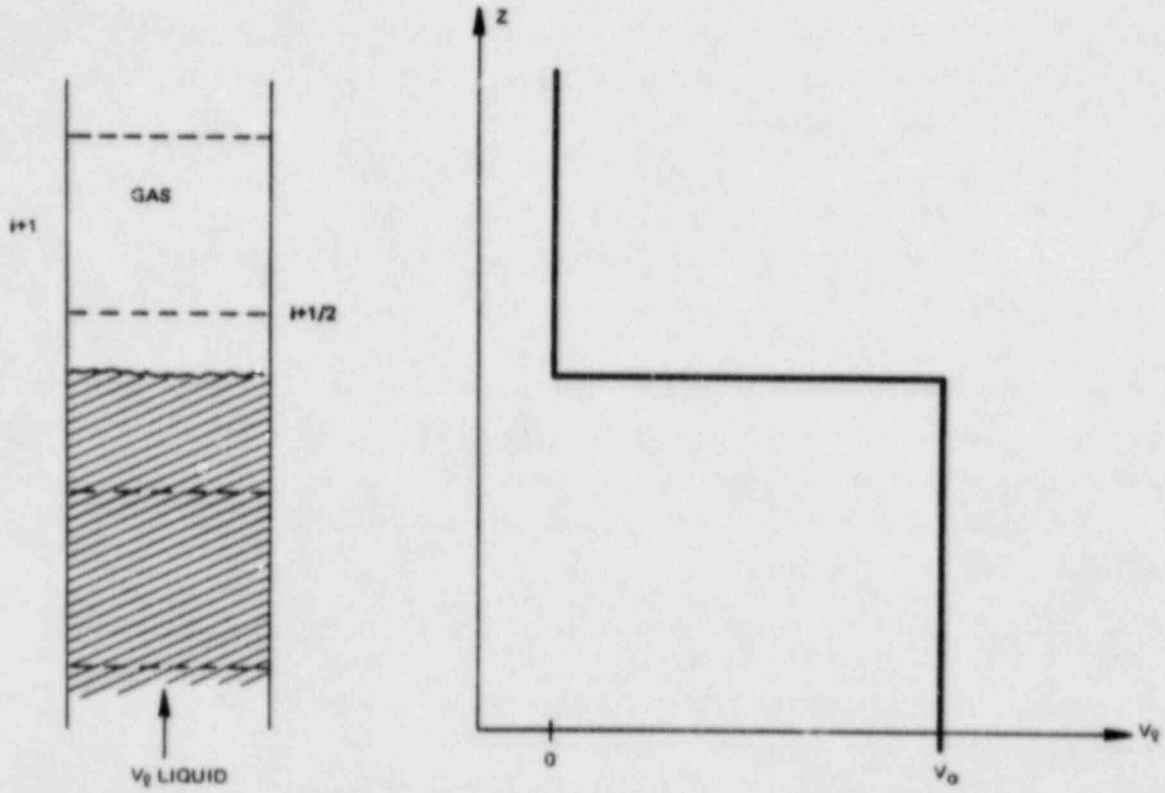

Figure 4-1. WATER PACKING

Figure 4-1 shows a case of rising water level that is notorious for producing water packing, especially if the liquid is subcooled. Below the level the liquid velocity is V_o and above the level the liquid velocity is zero. If condensation at the level was present, the liquid velocity above the level would be negative.

The liquid velocity as function of elevation is plotted in Figure 4-1 and it is seen that a discontinuity or jump in the liquid velocity exists at the level. This discontinuity moves upward with the velocity V_o.

With a finite discretization in space as shown on Figure 4-1, the velocity at boundary i + ½ would be zero until the level crosses the boundary and then it would be V_o. If the time step size is Δt and the node length is Δz, the pressure difference between cell i and i + 1 necessary to change the liquid velocity from zero to V_o in one time step will be:

$$\Delta P = \frac{\Delta z}{2} \rho_\ell \frac{V_o}{\Delta t} \qquad (4\text{-}1)$$

Typical numbers of $\Delta z = 1.0$m, $\rho_\ell = 1000$ kg/m^3, $V_o = 1$ m/sec and $\Delta t = 10^{-3}$ sec, result in $\Delta P = 5.0 \times 10^5$ Pa. A pressure spike of this magnitude is sufficient to significantly perturb the execution of any code. Furthermore, reduction of the time step size, just makes the problem worse.

This phenomenon can occur whenever a discontinuity exists. In practice, however, it is only a problem when the void approaches zero, where the inertia is high and the compressibility is low.

A possible solution would be to reduce the node size Δz to better simulate the fact that the liquid velocity actually changes over an in finitesimally short distance. However, that would increase the number of mesh cell to the point of making the cost of the calculations prohibitive. Thus, special messures are needed to resolve this problem of water packing.

If the void fraction and liquid velocity change continuously as function of the axial distance, the void and liquid velocity at boundary i + ½ would behave as indicated in Figure 4-2.

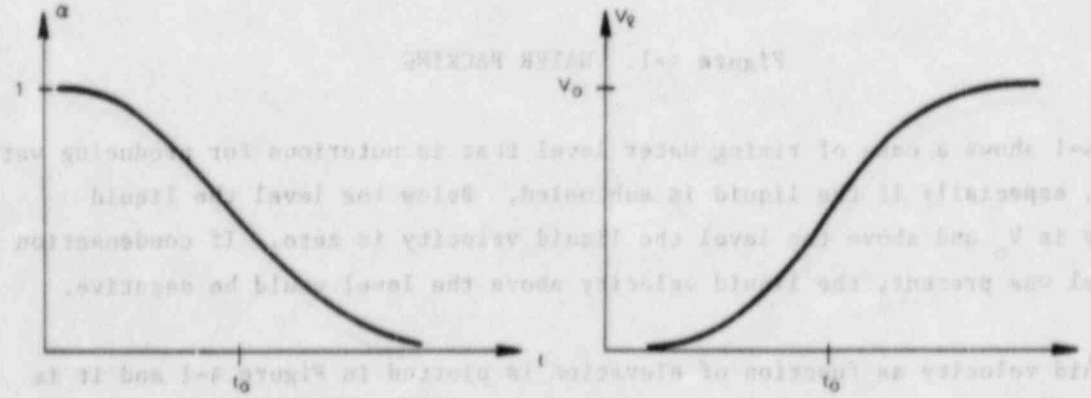

Figure 4-2. CONTINUOUS CHANGE IN NODAL PROPERTIES

In this case, no problems exist for the numerical integration since the properties are continuous.

For a discontinuity, the void fraction and liquid velocity and boundary $i + \frac{1}{2}$ change as indicated in Figure 4-3.

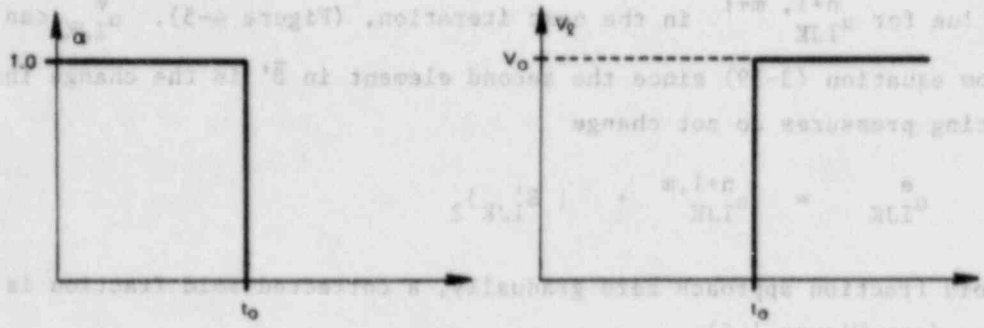

Figure 4-3. DISCONTINUOUS VARIATION IN NODAL PROPERTIES

In this case, the water packing phenomenon occurs.

One way of dealing with this problem, which was previously used in TRAC, was to reduce the liquid inertia by some large factor (typically 10^6) if a pressure spike was detected. This had the effect of allowing a change in the liquid velocity for a very small ΔP. This worked in most cases but sometimes tended to lock the pressure to a constant value. Furthermore, this solution was only implemented for internal boundaries, and not for junctions between components.

A different approach, which has been very successful, is to ensure that as the void fraction approaches zero, it does so continuously.

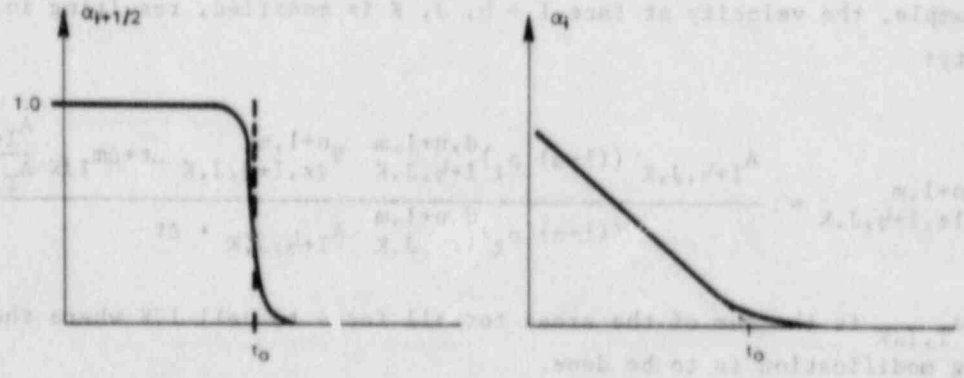

Figure 4-4. MODIFICATION TO DISCONTINUOUS VARIATION PROPERTIES WITH WATER PACKING LOGIC

As the liquid level approaches boundary i + ½, the void in cell i will gradually drop to zero. However, $\alpha_{i+\frac{1}{2}}$ changes abruptly from one to zero when α_i reaches zero. By smoothing out this transition as indicated in Figure 4-4, the water packing can be eliminated. This is accomplished through a modification to the momentum equation.

Let $\alpha_{IJK}^{n+1,\,m}$ be the latest value for the void fraction in cell IJK and α_{IJK}^{e} an estimated value for $\alpha_{IJK}^{n+1,\,m+1}$ in the next iteration, (Figure 4-5). α_{IJK}^{e} can be obtained from equation (3-39) since the second element in $\bar{B}'$ is the change in α if the neighboring pressures do not change

$$\alpha_{IJK}^{e} = \alpha_{IJK}^{n+1,m} + \{ B'_{IJK} \}_2 \tag{4-2}$$

Tolet the void fraction approach zero gradually, a corrected void fraction is calculated as (see Figure 4-5):

$$\alpha_{IJK}^{c} = \alpha_{IJK}^{n+1,m} \exp \left(- \frac{\alpha_{IJK}^{n+1,m} - \alpha_{IJK}^{e}}{\alpha_{IJK}^{n+1,m}} \right) \tag{4-3}$$

This modification is chosen as it results in a continuous variation in α, has a continuous slope at iteration m, and it approaches zero asymptotically at iteration m + 1.

For iteration m + 1 to give in $\alpha_{IJK}^{n+1,m+1} = \alpha_{IJK}^{c}$ more liquid must be removed from cell IJK. The amount is:

$$\Delta m_{IJK} = \Psi_{IJK}\, \rho_{\ell}\, (\alpha_{IJK}^{c} - \alpha_{IJK}^{e}) \tag{4-4}$$

This is accomplished by modifying the liquid velocities at the faces of cell IJK. For example, the velocity at face I + ½, J, K is modified, resulting in the new velocity:

$$V_{lz,I+\frac{1}{2},J,K}^{n+1,m} = \frac{A_{I+\frac{1}{2},J,K}\, ((1-\alpha)\, \rho_{\ell})_{I+\frac{1}{2},J,K}^{d,n+1,m}\, V_{\ell z,I+\frac{1}{2},J,K}^{n+1,m}\, \Delta t + \Delta m_{IJK}\, \frac{A_{I+\frac{1}{2},J,K}}{A_{T,IJK}}}{((1-\alpha)\, \rho_{\ell})_{I+\frac{1}{2},J,K}^{d,n+1,m}\, A_{I+\frac{1}{2},J,K} \cdot \Delta t} \tag{4-5}$$

where $A_{T,IJK}$ is the sum of the areas for all faces to cell IJK where the water packing modification is to be done.

Here it is worth noting that with the exponential chosen in Equation (4-3) $\Delta m \sim \Delta t^2$, i.e. the modification to the velocity goes to zero as Δt goes to zero.

The water packing logic is turned on if the following conditions are met.

$$\alpha_{IJK} \to 0 \quad (\alpha^e_{IJK} < \alpha^{n+1,m}_{IJK} \quad \text{and} \quad \alpha^e_{IJK} < 0.09)$$

$$\alpha_{neighbor} > 0.1 \text{ for at least one neighboring cell.}$$

i.e. the void fraction in cell IJK is approaching zero and there is room for the extra liquid removed from cell IJK in one of the neighboring cells. It should be noted that with the second criteria, the capability of the code to predict water hammer is not affected.

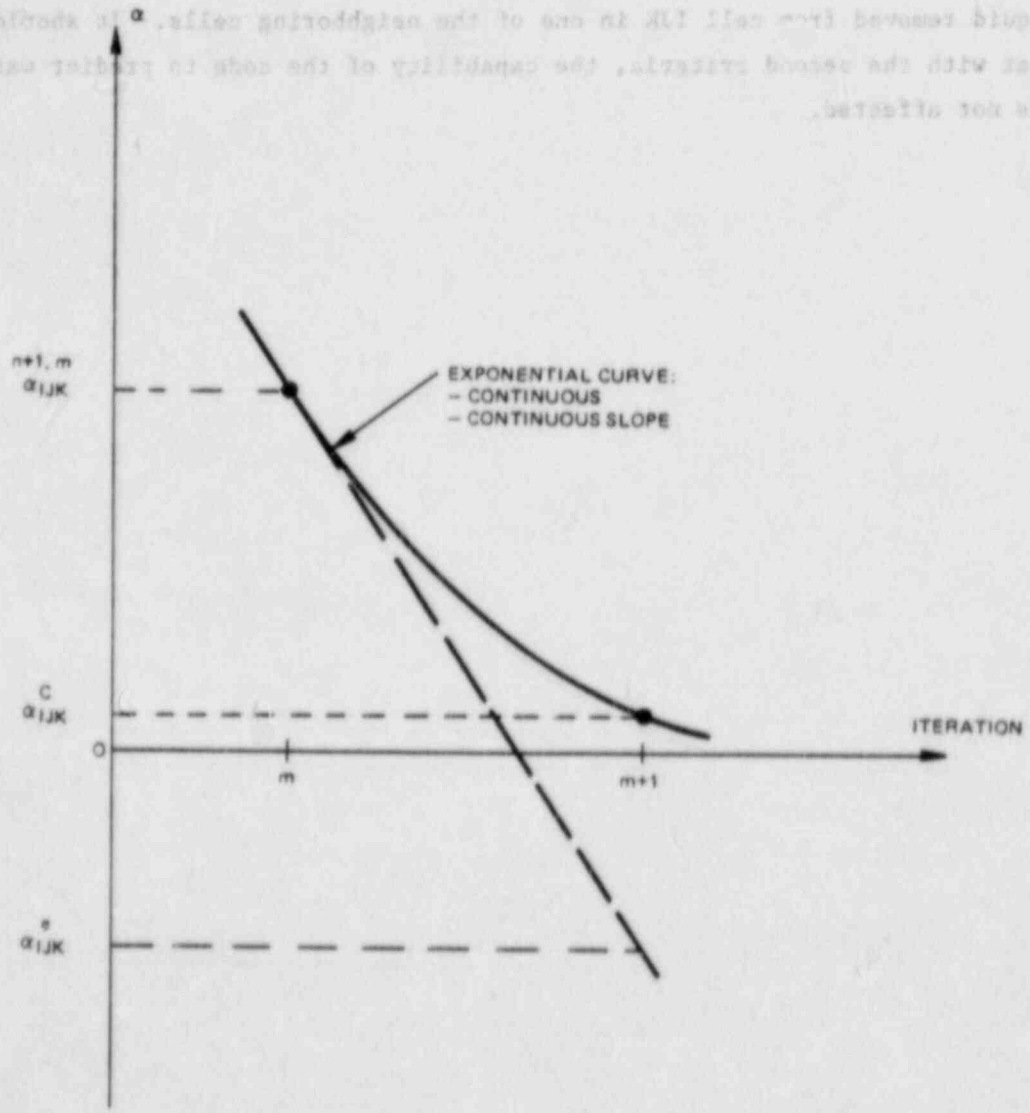

Figure 4-5. WATER PACKING MODIFICATIONS TO VOID FRACTIONS

SECTION 5

DEVELOPMENT ASSESSMENT

The developmental assessment of the fast numerics for the 3D component in TRACB04 has included testing for correct implementation and validation to demonstrate the performance of the fast numerics. Typical examples on this testing will be shown in this section.

5.1 TESTING FOR CORRECT IMPLEMENTATION

The testing for correct implementation of the first numerics has included two types of testing. For cases where only one dimension of the vessel component is utilized, it is possible to compare with the fast numerics for the one dimensional component, which was developed for TRACB03. In performing this comparison, a temporary edit was implemented into TRAC and the individual matrix elements were printed out. Exact agreement was not expected due to minor differences in the implementation of constitutive correlations for the 1D and 3D components, but very close agreement should exist. An example of such a comparison is shown in Table 5-1 for a case of a flowing two phase-mixture of approximately 50% void fraction. It is seen that the difference is in the order 0.01% or less, which is judged to be acceptable in light of the mentioned differences between 1D and 3D components. This type of comparison was conducted using both very small and very large time steps whereby both the time step invariant part and time step dependent part of the matrix elements could be tested individually.

For cases where several dimensions in the 3D component were used simultaneously, the testing was conducted by comparing the fast numerics to the old semi-implicit numerics for the 3D component. Again, exact agreement is not expected since significant differences existed in the implementation of the constitutive correlations between the 1D and 3D components for the old numerical method, particularly for the interfacial heat transfer. An important part of the implementation of the fast numerics for the 3D component was that the formulation of the basic equations and the solution method as far as possible was made consistent with the 1D component. Consequently as stated, exact agreement between old and new method is not expected, but similar results should be obtained. An example of such a comparison is shown in Figure 5-1 and 5-2. In the test case, a two-phase mixture with 50% void fraction was injected in cell 5 and extracted from cell 8. The fluid would simultaneously flow in two directions, the radial and the azimuthal. Due to the centrifugal force on the fluid,

the liquid would tend to collect in the outer ring, whereas the vapor would primarily flow in the inner ring. This is seen in Figure 5-2 where the void fraction in cell 6 is compared for the two calculations. The void in the vessel was initialized at a value of 50% and after going through a transient, the void in cell 6 reaches a final value of 31%. This is seen in both cases. However, in the case of the fast numerics, the transition is seen to be somewhat slower. This is a result of the numerical diffusion inherent in the more stable implicit numerical methods, when large times steps are taken.

Table 5-1

COMPARISON OF 'A' MATRIX FOR 1D AND 3D FAST NUMERICS

ACOEF	1D VALUES	3D VALUES	% DIF.
1,1	3.950678E-06	3.951298E-06	0.016
2,1	5.060848E-06	5.060746E-06	-0.002
3,1	9.363116E+00	9.363813E+00	0.007
4,1	1.003686E+01	1.003665E+01	-0.002
5,1	0.0	0.0	
1,2	3.640277E+01	3.640205E+01	-0.002
2,2	-7.055904E+02	-7.055763E+02	-0.002
3,2	1.009908E+08	1.009887E+08	-0.002
4,2	-8.388447E+08	-8.388279E+08	-0.002
5,2	0.0	0.0	
1,3	1.100845E-01	-1.101546E-01	0.064
2,3	-1.099909E-01	-1.099886E-01	-0.002
3,3	-2.138908E+05	-2.136963E+05	-0.091
4,3	-2.134902E+05	-2.134859E+05	-0.002
5,3	0.0	0.0	
1,4	-3.317188E-04	-3.317187E-04	-0.000
2,4	-1.105353E+00	-1.105331E+00	-0.002
3,4	-9.202743E+02	-9.203746E+02	0.011
4,4	5.987460E+05	5.987340E+05	-0.001
5,4	0.0	0.0	
1,5	-8.351036E-07	-8.357871E-07	0.082
2,5	-8.309857E-07	-8.309691E-07	-0.002
3,5	-8.118153E+00	-8.118881E+00	0.009
4,5	-8.108095E+00	-8.107933E+00	-0.002
5,5	1.0	3.115511E-06	*not relevant

*Comparison is not relevant since TFIDI value is reset to 1.0 when no air is present.

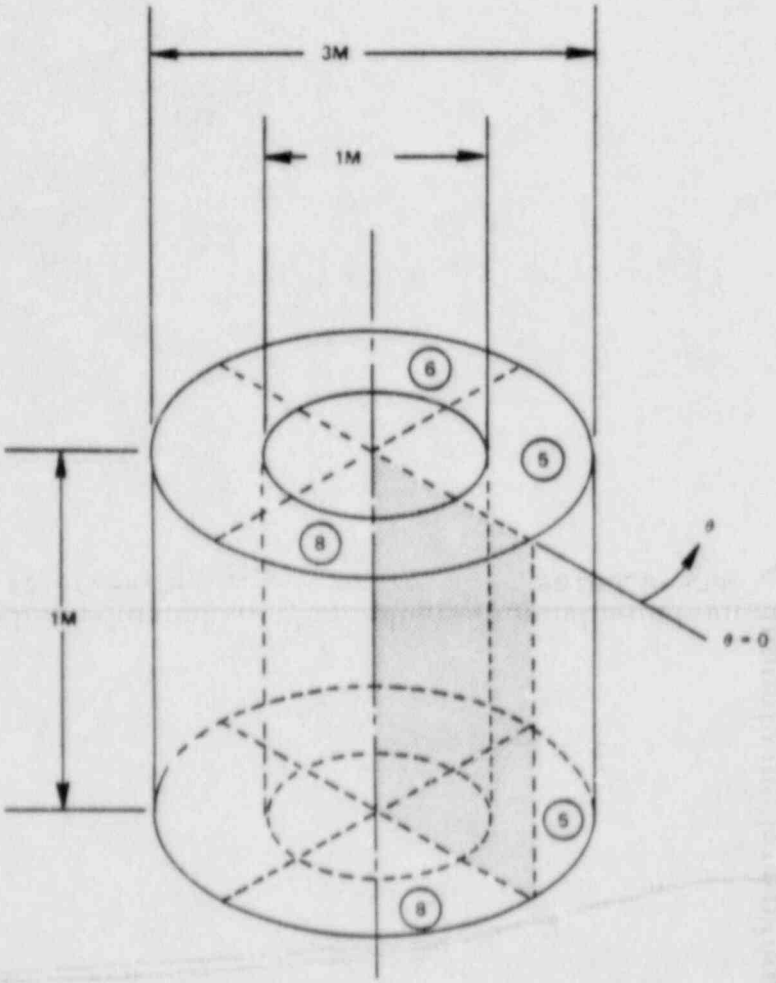

Figure 5-1. SINGLE-LEVEL, TWO-RING, FOUR-SECTION VESSEL

Cross-hatched face is blocked, i.e. flow area in azimuthal direction is zero. Shaded face is also blocked; however, both PIPE 1Ø and PIPE 2Ø each with a flow area of $1m^2$ are attached normal to the shaded face so that the FILL adds mass to cell #5 and the BREAK removes mass from cell #8. PIPE 1Ø and PIPE 2Ø both contain a single cell one meter in length.

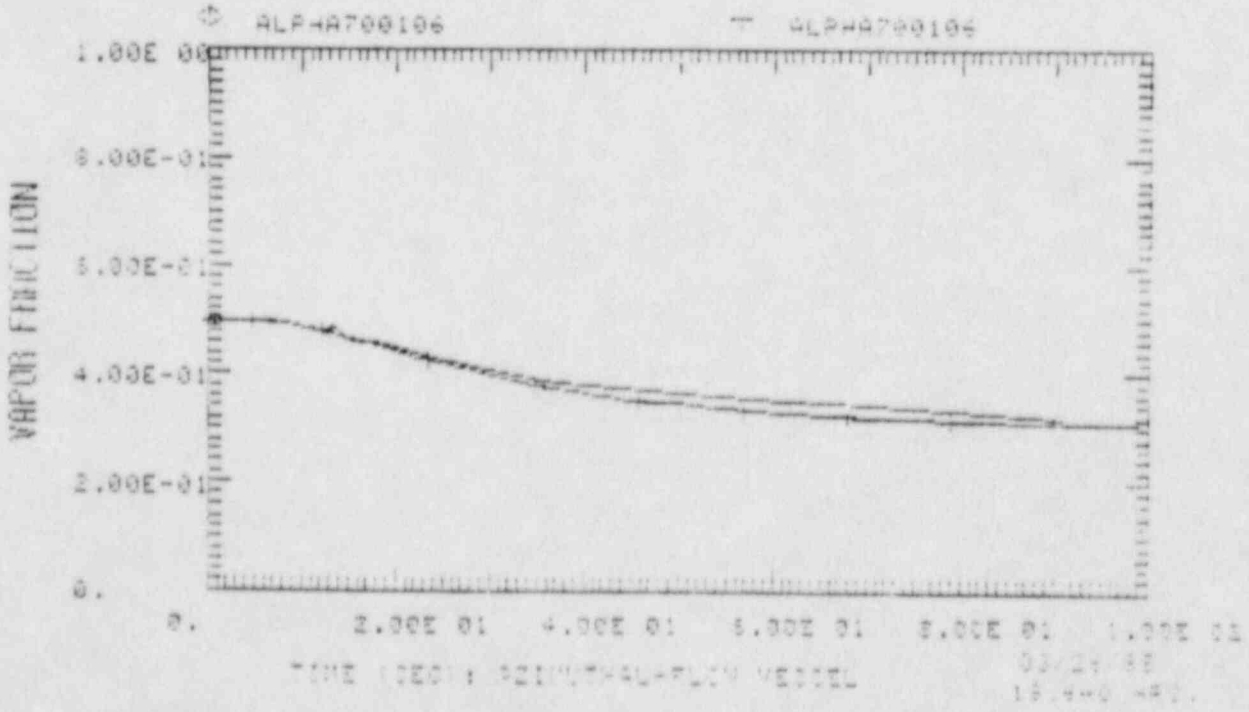

Figure 5-2. COMPARISON OF FAST AND SEMI-IMPLICIT METHODS

Good agreement in the final value is observed, but differences exist during the transient. Care must be taken during transients to control the time step size such that any numerically introduced error remains at an acceptable level.

Based on these results, it has been concluded that the fast numerics for the 3D component in TRAC has been correctly implemented.

5.2 PERFORMANCE TESTING OF FAST NUMERICS

In order to determine how much could be gained in execution time from the fast numerics, i.e., how much the time step size can be increased without a significant reduction in the accuracy of the simulation and what this means for the overall execution time, TRACB04 has been compared to the PSTF blowdown test 5803-01. (Figure 5-3 through 5-9.) The geometry of the PSTF test is shown in Figure 5-3 and the TRAC nodalization is shown in Figure 5-4. A vessel component was used to simulate the PSTF vessel and a pipe component was used for the break pipe.

Two calculations were conducted with an upper limit on the time step (CMULT) of 100 and 400 times the material Courant limit. The time steps used in the two calculations are shown in Figure 5-5. For comparison, the old numerical method used time steps in the order of 1-2 msec. Initially, while the level is dropping the time step is controlled by the rate of change for the void fraction in the cell containing the level. As the break pipe is uncovered and a rapid change in the break flow takes place, the time step is temporarily reduced to a low value in the order of the material Courant limit. This is to be expected since an accurate calculation of fast changes requires small time steps. However, as the levels drop below the break pipe and the break flow is essentially single phase steam, property changes become more sedate again and the time step size quickly increases to its maximum allowed value. This is clearly seen for the case of CMULT = 100. For CMULT = 400, the time step is intermittently controlled by the rate of change in the vessel pressure. Consequently, a further increase in CMULT would not significantly increase the achieved time step size.

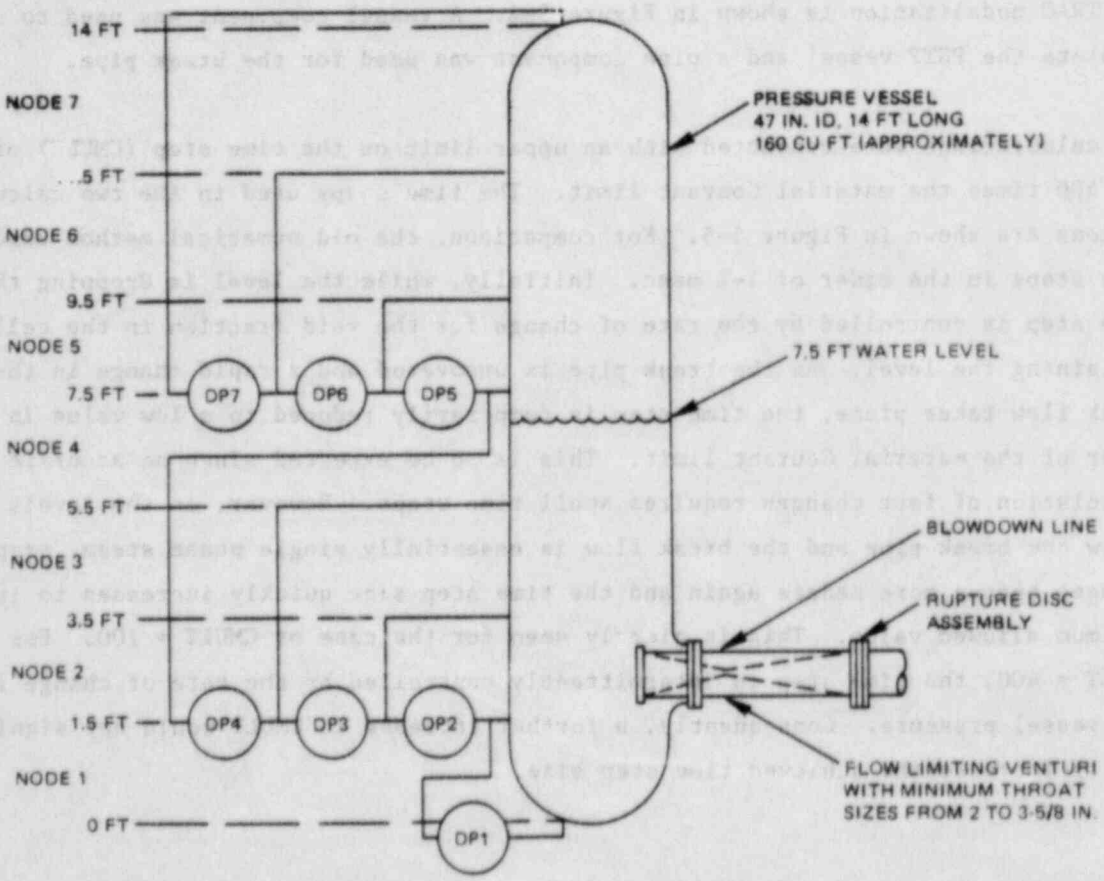

Figure 5-3. PSTF TEST 5803-01

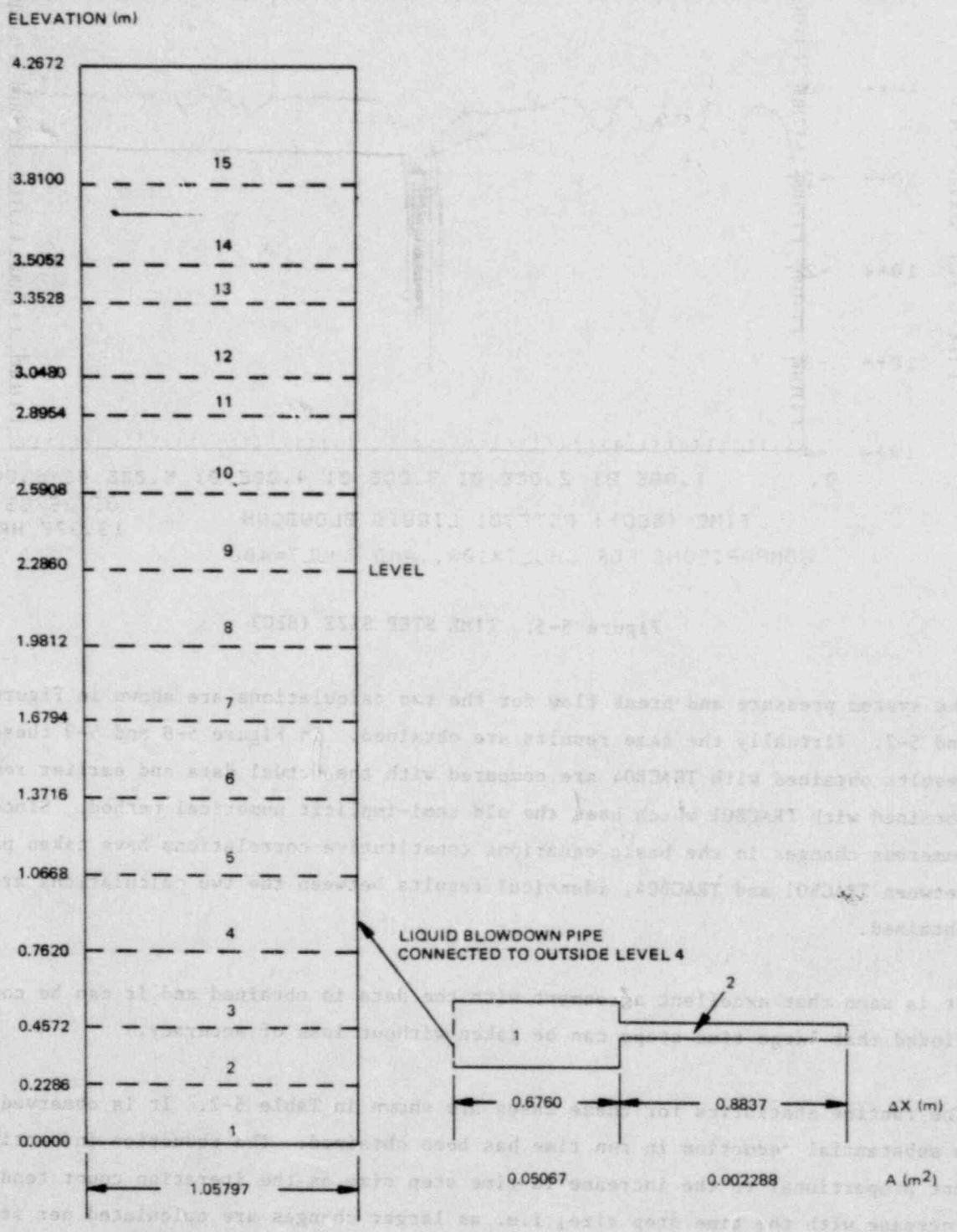

Figure 5-4. TRAC MODEL FOR PSTF

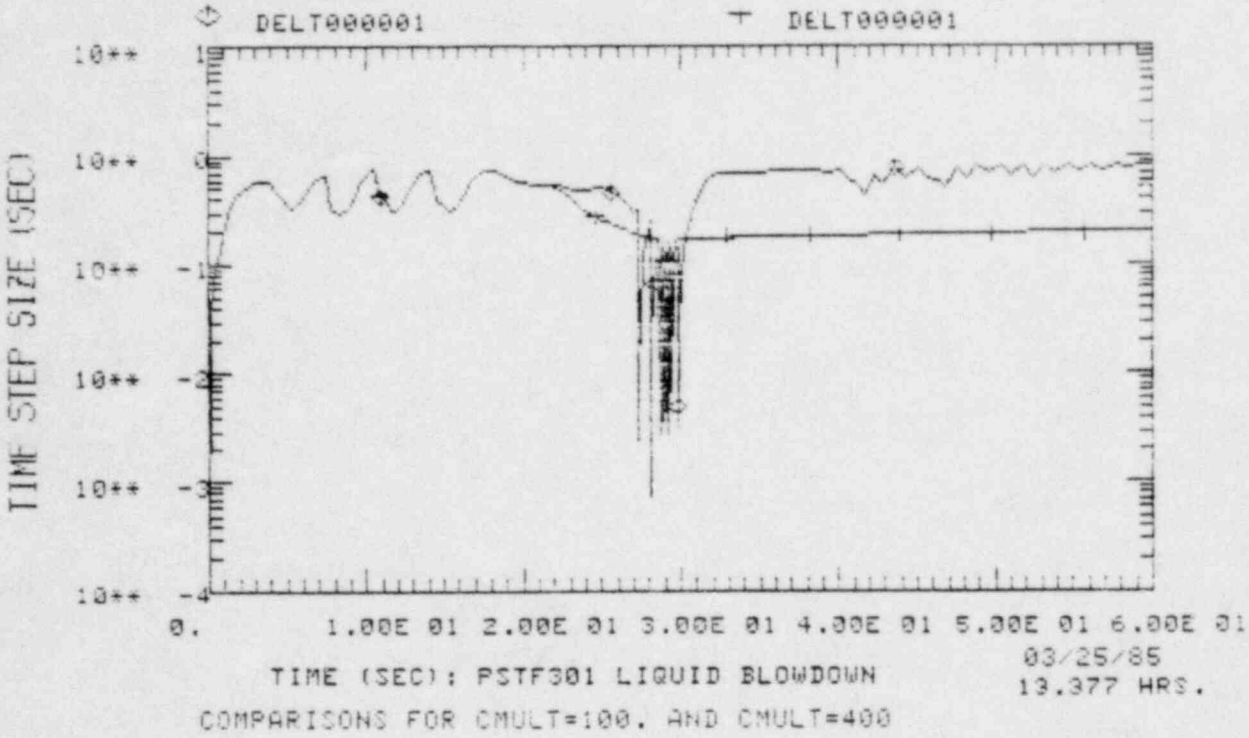

Figure 5-5. TIME STEP SIZE (SEC)

The system pressure and break flow for the two calculations are shown in Figures 5-6 and 5-7. Virtually the same results are obtained. In Figure 5-8 and 5-9 these results obtained with TRACB04 are compared with the actual data and earlier results obtained with TRACB01 which uses the old semi-implicit numerical method. Since numerous changes in the basic equations constitutive correlations have taken place between TRACB01 and TRACB04, identical results between the two calculations are not obtained.

It is seen that excellent agreement with the data is obtained and it can be concluded that large time steps can be taken without loss of accuracy.

The runtime statistics for these cases are shown in Table 5-2. It is observed that a substantial reduction in run time has been obtained. The reduction in runtime is not proportional to the increase in time step size as the iteration count tends to increase with the time step size, i.e. as larger changes are calculated per step, more iterations are needed for convergence. However, the advantages of longer time steps clearly outweighs the cost of additional iterations giving a large overall gain.

Table 5-2

EXECUTION STATISTICS FOR PSTF LIQUID BLOWDOWN

CASE	Semi-implicit numerics (TRACB01)	Fast implicit numerics (TRACB04)	Fast implicit numerics (TRACB04)
CMULT	1.0	100.	400.
Execution time	1309.0	84.31	66.06
Problem time	39.50	60.12	60.06
Execution/problem time	33.14	1.40	1.01
Execution/problem time for last 20 seconds	66.0*	1.40	0.424

*For last two seconds of problem

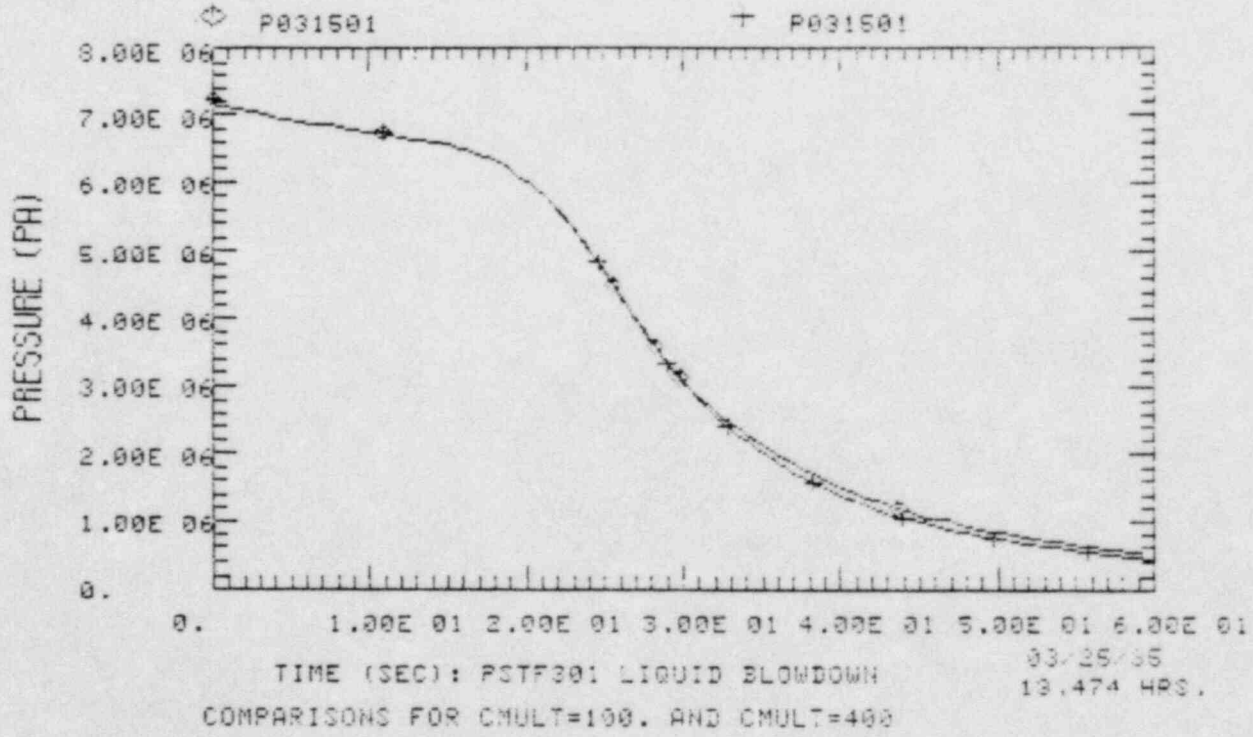

Figure 5-6. PRESSURE (PA)

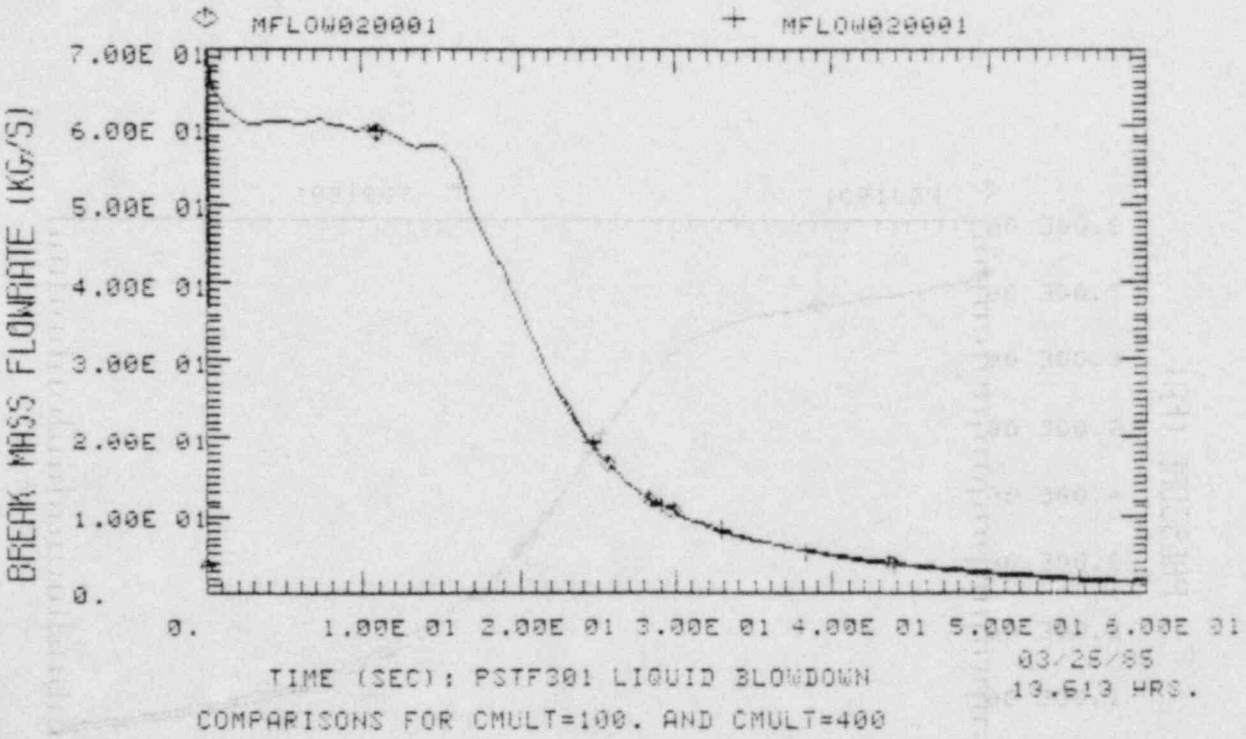

FIGURE 5-7. BREAK MASS FLOWRATE (KG/S)

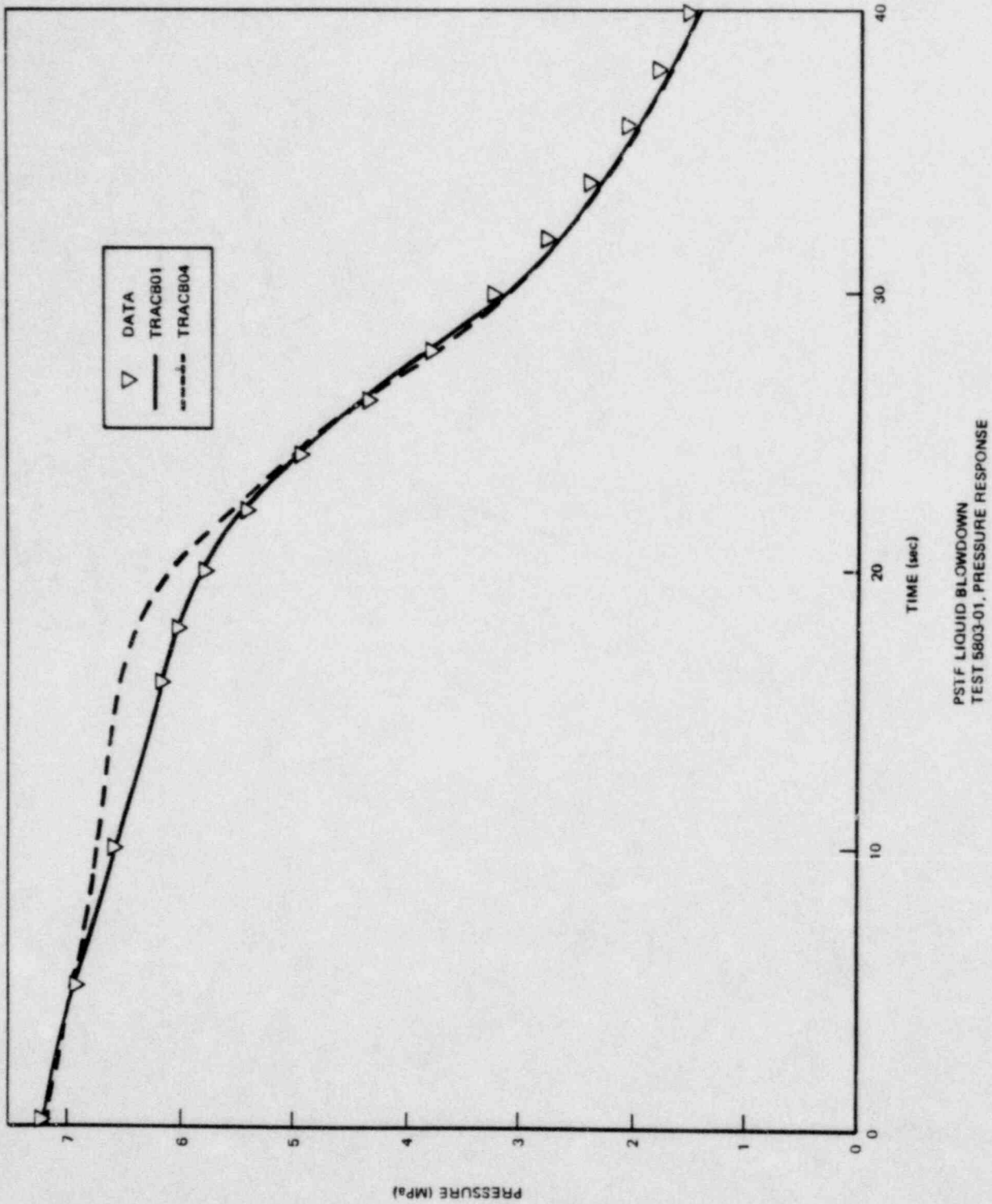

Figure 5-8. PSTF LIQUID BLOWDOWN TEST 5803-01: PRESSURE RESPONSE

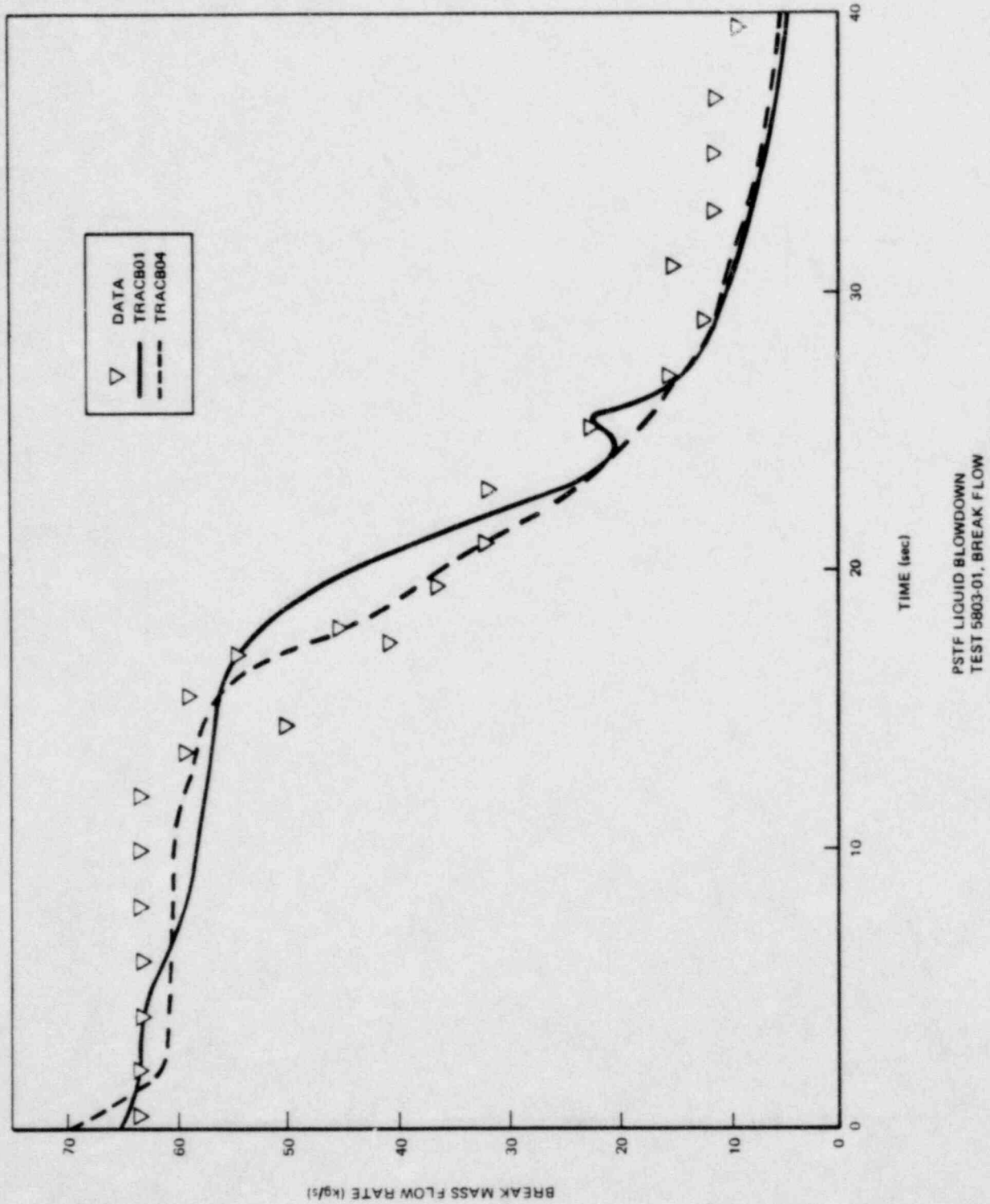

Figure 5-9. PSTF LIQUID BLOWDOWN TEST 5803-01: BREAK FLOW

SECTION 6
CONCLUSION

A fast implicit numerical method has been developed and implemented for the 3D component in TRACB04. Together with the fast numerics developed earlier for the 1D components in TRACB, the fast numerics scheme is available for the entire hydraulic model in TRAC. Consequently, the time step size is no longer limited by the material Courant limit, but by the accuracy of the calculation.

The fast numerics has been extensively tested and it has been demonstrated that the model is correctly implemented and that a large reduction in execution time can be obtained particularly for slow transients without loss of accuracy.

SECTION 7

REFERENCES

(1) Andersen, J.G.M., Chu, K.H., Shaug, J.C.; BWR Refill-Reflood Program Task 4.7 - Model Development Basic Models for the BWR Version of TRAC (NUREG/CR-2573, EPRI NP-2375, GEAP-22051); September 1983.

(2) Andersen, J.G.M. and Chu, K.H.; BWR Refill-Reflood Program Task 4.7 - Constitutive Correlations for Shear and Heat Transfer for the BWR Version of TRAC (NUREG/CR-2134, EPRI NP -1582, GEAP-24940); December 1981.

(3) Weaver, W.L., III; TRAC-BWR Completion Report [for] Noncondensible Gas Model (WR-CD-82-062); EG&G Idaho, Inc.; January 1983.

(4) Liles, D.R., et al; TRAC-PF1: An Advanced Best-Estimate Computer Program for PWR Analysis; Safety Code Development Group, Energy Division; LASL; 1981.

(5) Spore, Jay W., et al; TRAC-BD1: An Advanced Best-Estimate Computer Program for Boiling Water Reactor Loss-of-Coolant Accident Analysis (NUREG/CR-2178, EGG-2109, Volumes 1-4); October 1981.

SECTION 8

NOMENCLATURE

Symbol	Unit	Description
A	m^2	Flow area
$\underline{\underline{A}}$	N/A	Matrix (Eq. 3.34)
$\bar{B}$	N/A	Vector (Eq. 3.34)
B	m/sec^2	Momentum source
C	-	Courant number
$\bar{C}$	N/A	Vector
$\bar{D}$	Pa	Vector (Eq. 3.53)
d	Pa	Coefficient (Eq. 3.48)
E	J/m^3 sec	Energy Source
$\underline{\underline{E}}$	-	Matrix (Eq. 3.53)
e	J/kg	Specific energy
$\bar{e}$	-	Vector (Eq. 3.48)
F	N/A	Vector (Eq. 3.32)
$\underline{\underline{F}}$	-	Matrix (Eq. 3.53)
F_w	kg/m^2 sec^2	Wall Friction
$f_{\ell g}$	kg/m^2 sec^2	Interfacial shear
$\underline{\underline{G}}$	-	Matrix (Eq. 3.58)
g	m/sec^2	Acceleration of gravity
h_i	J/kg -	Specific enthalpy Imaginary unit
Ja	N/A	Jacobian Matrix
k	m^{-1}	Wave number
k	-	Virtual mass coefficient
M	kg/m^3 sec	Mass source
m	kg	Mass
P	Pa	Pressure

NOMENCLATURE (Continued)

Symbol	Unit	Description
q	W/m^3	Volumetric heat flux
R	m	Radial dimension
Sc	N/A	Vector (Eq. 3.34)
T	K	Temperature
t	sec	Time
V	m/s	Velocity
$\forall$	m^3	Volume
x	m	Length
z	m	Axial dimension

Greek Symbols

Symbol	Unit	Description
α	-	Void fraction
ϕ	N/A	Parameter (Eq. 3.1)
ρ	kg/m^3	Density
λ	-	Amplification factor
Γ	kg/m^3 sec	Vapor generation rate
θ	-	Azimuthal dimension

Subscripts

Symbol	Description
a	Air
c	Continuous phase
d	Dispersed phase
g	Gas
i	Index
I	Axial index
j	Index
J	Radial index
K	Azimuthal index
ℓ	Liquid
R	Radial
R	Relative
s	Saturated
w	Wall
z	Axial
θ	Azimuthal

Superscripts

Symbol	Description
d	Donor cell
m	Iteration count
n	Time step

NRC FORM 335 (2-84) NRCM 1102, 3201, 3202

U.S. NUCLEAR REGULATORY COMMISSION

BIBLIOGRAPHIC DATA SHEET

SEE INSTRUCTIONS ON THE REVERSE

1. REPORT NUMBER (Assigned by TIDC, add Vol. No., if any)
NUREG/CR-4127, Vol. 1
EPRI NP-3987
GEAP-30875

2. TITLE AND SUBTITLE
BWR Full Integral Simulation Test (FIST) Program
TRAC-BWR Model Development
Volume 1: Numerical Methods

3. LEAVE BLANK

4. DATE REPORT COMPLETED
MONTH: April
YEAR: 1985

5. AUTHOR(S)
C.L. Heck, J.G.M. Andersen

6. DATE REPORT ISSUED
MONTH: November
YEAR: 1985

7. PERFORMING ORGANIZATION NAME AND MAILING ADDRESS (Include Zip Code)
General Electric Company
Nuclear Technology and Fuel Division
175 Curtner Avenue
San Jose, CA 95125

8. PROJECT/TASK/WORK UNIT NUMBER

9. FIN OR GRANT NUMBER
B3014

10. SPONSORING ORGANIZATION NAME AND MAILING ADDRESS (Include Zip Code)
Division of Accident Evaluation
Office of Nuclear Regulatory Research
U.S. Nuclear Regulatory Commission
Washington, D.C. 20555

11a. TYPE OF REPORT
Technical

b. PERIOD COVERED (Inclusive dates)

12. SUPPLEMENTARY NOTES

13. ABSTRACT (200 words or less)

A complete technical basis for implementation of the 3-D fast numerics in TRACB04 is presented. The 3-D numerics is a generalization of the predictor/corrector method previously developed for the 1-D components in TRACB.

14. DOCUMENT ANALYSIS - a. KEYWORDS/DESCRIPTORS
Boiling Water Reactor (BWR)
Loss-of-Coolant Accident (LOCA)
Full Integral Simulation Test (FIST)
Transient Reactor Analysis Code (TRAC)

b. IDENTIFIERS/OPEN-ENDED TERMS

15. AVAILABILITY STATEMENT
Unlimited

16. SECURITY CLASSIFICATION
(This page) Unclassified
(This report) Unclassified

17. NUMBER OF PAGES

18. PRICE